

Automated Analysis of Room Performance

Michael Novak

June 3, 2012

Appendix A

Data

- Postmortem data gotten from `/u/karavan/Public` at `rita.cat.pdx.edu`
- 2011-05-05—The Low Density Workload—LD_A1_56p_2ppn_28n_I0-BASIC_even_RAWDATA
- 2011-04-25—The High Density Workload—HD_A1_224p_8ppn_28n_RAWDATA
- This data seems to correspond to the experiments in [2].
- [2, p. 436]

In the HD schedules, the 224 processes ran on 28 nodes (eight processes per node) all housed in a single rack.

- [2, p. 436]

In the low density LD schedules, the 224 processes executed on 112 nodes, with two processes per node, and the processes were spread across racks B1, B2, B3, and B4.

- [2, p. 436]

Low Density Even Distribution – In this set, we used racks B1, B2, B3, and B4; and we scheduled two MPI tasks per node, using all of the nodes in all four racks.

- [2, p. 436]

The nodes are connected via a DDR InfiniBand 1-layer fat tree; one rack (A2) contains the networking equipment and seven racks (A1, A3–4, B1–4) are for the compute nodes.

- [2, p. 437]

Power. We collect power per rack, at 10 second intervals. This is converted by FRED to kWh.

- [2, p. 437]

Cooling. Each spray-cooled rack has a Thermal Management Unit (TMU) which contains pumps, a liquid-to-liquid heat exchanger, and control electronics.

- [2, p. 436]

All of the power and cooling data measured by FRED [Fundamental Research in Energy efficient Data centers, an analysis software tool developed at PNNL] sensors is collected into a central FRED database, using an independent data network. This is significant because the room environment data collection does not perturb the running application, and the data itself does not drive up the scaling requirements for the application performance measurement tool.

- The application and system level data for each trial (t01–03) are in the trial directories: t1, t2, t3 (we don’t really need this information).

A.1 Power & Cooling

Tables in Appendix B show power consumption, in kWh (7.63¢ per kWh, in Oregon), for the racks used in the LD and HD trials. Note: the data is badly corrupted by faulty sensor readings; especially for node-level temperature readings for CPUs and air, which gave negative, and ludicrously high, temperature values—these false readings had to be filtered from the true readings. For CPU temperature the filtering range was $72 < temp < 150$; for Node air temperature the filtering range was $0 < temp < 40$. So the average temperatures do not include every node in every rack; see the node counts.

The figures in Appendix C include TMU utilization for each : the degree of cooling which the TMU provided, captured by the water-temperature-delta metric; and the mass flow rate of water, captured by the manifold pressure metric. TMU utilization metrics were collected by FRED at 10 second intervals; so, for simplicity, each trial’s time series starts at 0 and is incremented accordingly.

Note: The TMU utilization metrics for the HD dataset were erroneous; hence Appendix E only includes figures for Chiller metrics.

A.2 Chillers

Within the cooling infrastructure, most of the energy is spent on chillers, which refrigerate the coolant—water, in our case—used to extract heat from the equipment in the data center. The following metrics, derived from [3], are displayed Appendix C & E. Chiller utilization measurements were collected by FRED at 30 second intervals; so, for simplicity, each trial’s time series starts at 0 and is incremented accordingly. Note: only three chillers units (C_1, C_2, C_4) were turned on during the trials, as evidenced by KW consumption— C_3 and C_5 were turned off.

- **IT cooling load.** This is the amount of heat that is generated (and thus needs to be dissipated) at a data center. It is approximately equivalent to the power consumed by the equipment since almost all of it is dissipated as heat. It is commonly specified in kilowatts (KW).
- **COP.** The coefficient of performance (COP) of a chiller unit indicates how efficiently the unit provides cooling, and, is defined as the ratio between the cooling provided and the power consumed, i.e.,

$$COP_i = \frac{L_i}{P_i} \tag{A.1}$$

where L_i is the cooling load on the i th chiller unit and P_i is the power consumed by it.

- **Chiller utilization.** Chiller utilization depends on the degree of cooling provided; i.e., the difference between the inlet and outlet water temperatures.

A.3 Data Mining

If only we had access to more data...

- It would be nice if FRED measurements were stored in a NoSQL graph database. A NoSQL database would be much faster than PostgreSQL. And having the data structured as a graph seems like it would make the data easier to navigate.
- We could compare high-density workload with low-density workload; and , perhaps medium-density workload—if it exists.
- The temporal data-mining technique of overlaying clusters on the time series, described in [3, 4], was tested on Chiller data. Though, it was difficult to find motifs at such a fine granularity, with our limited data.
- [4, p. 34:7]

Motifs are repetitive patterns of occurrence in time-series data. In understanding multivariate time-series data about chiller utilizations, we seek to identify motifs that underly how different chillers are involved in meeting the varying demand posed by data centers. We would like to identify regions of time-series progression that demonstrate better/improved sustainability measures than others.

- [3, pp. 1308–1309]

A multivariate time series $T = \langle t_1, \dots, t_m \rangle$ is an ordered set of real-valued vectors of a particular variable. Each real-valued vector t_i captures the utilizations across all the chiller units.

- You look at the time series to detect motifs, then see if they are captured by clustering.
- [4, p. 34:12]

First, the time information is stripped from the data and clustering is performed with number of clusters, $k = 5$. The cluster transitions are overlaid in the plot. These transitions are used to encode the multivariate numeric data into symbolic form and serve as the input to frequent episode mining. One episode is discovered which occurs five times and this episode is unpacked into the original data and overlaid on the dataset as shown. This serves as an example of a motif that we embedded and were able to uncover.

[4, p. 34:6] High amplitude and frequent variations in utilization due to varying load or some failure condition result in decreased lifespan, and, thus, need to be minimized.

- Algorithms can be developed for processing multivariate time-series data to characterize sustainability measures of the patterns mined.

For clustering, I'm using ELKI (release 0.4.1 [1]). The algorithms being used are: k -means and expectation maximum (EM). Gaussian clusters discovered by EM clustering with $k = 3$, over the three trials for the Chiller metrics, produced the best results. I've labelled the input data in such a way that the time-series information is retained after clustering; so the cluster transition can be overlaid in their corresponding plot. Naively thinking the three trials for each workload (LD & HD) could be clustered on their chiller metrics led to the automated analysis captured in the cluster-overlaid time-series figures in Appendix D & F. Meaningful clustering could be done with more data; as, for example, done in [4, pp. 34:14–34:16 (see Tables I–V)].

Appendix B

Tables for Per-Node Energy Metrics

Low-Density Workload

PowerUnit	PowerKWH	A1	A3	A4	B1	B2	B3	B4
	t01	1.28	1.03	1.07	1.11	1.17	1.31	1.27
	t02	1.28	1.03	1.06	1.11	1.17	1.31	1.27
	t03	1.30	1.05	1.09	1.13	1.19	1.33	1.35
Total	PowerUnit	1	1	1	1	1	1	1

Total kWh increase.

CPU Temp	A1	A3	A4	B1	B2	B3	B4
t01	90.49	82.88	82.94	99.91	90.40	101.47	108.81
t02	90.49	82.88	82.94	99.91	90.40	101.47	108.81
t03	90.49	82.88	82.94	99.91	90.40	101.47	108.81
Total CPU	37	40	4	5	6	4	5

Average Per-Node, Per-CPU, CPU Temperature Average for Each Rack (within $72 < \text{Temp} < 150$)

CPU Temp	A1	A3	A4	B1	B2	B3	B4
t01	92.61	141.70	85.69	127.22	92.47	112.55	114.63
t02	92.61	141.70	85.69	127.22	92.47	112.55	114.63
t03	92.61	141.70	85.69	127.22	92.47	112.55	114.63
Total CPU	37	40	4	5	6	4	5

Maximum Per-Node, Per-CPU, CPU Temperature Maximum for Each Rack (within $72 < \text{Temp} < 150$)

NodeAir Delta	A1	A3	A4	B1	B2	B3	B4
t01	26.10	24.44	26.30	25.51	24.55	23.51	26.39
t02	26.10	24.44	26.30	25.51	24.55	23.51	26.39
t03	26.10	24.44	26.30	25.51	24.55	23.51	26.39
Total NodeAir	24	24	22	25	23	23	16

Average Per-Node Air Temperature Delta for Each Rack (within $0 < \Delta\text{Temp} < 40$)

High-Density Workload

PowerUnit	PowerKWH	A1	A3	A4	B1	B2	B3	B4
	t01	13.35	9.89	10.24	10.73	11.12	13.07	14.34
	t02	6.87	4.25	4.41	4.56	4.86	5.69	6.14
	t03	18.90	12.08	12.48	12.95	13.73	16.13	17.51
Total	PowerUnit	1	1	1	1	1	1	1

Total kWh increase.

CPU Temp	A1	A3	A4	B1	B2	B3	B4
t01	97.18	83.52	81.71	100.15	89.51	94.54	110.43
t02	104.83	83.99	82.30	100.44	89.75	94.22	111.05
t03	116.73	83.89	82.26	100.42	89.68	97.33	111.66
Total CPU	37	41	4	5	6	4	5

Average Per-Node, Per-CPU, CPU Temperature Average for Each Rack (within $72 < \text{Temp} < 150$)

CPU Temp	A1	A3	A4	B1	B2	B3	B4
t01	107.68	141.97	85.05	127.94	91.73	106.14	120.02
t02	126.13	142.13	85.20	127.94	91.86	106.93	120.95
t03	126.13	142.13	85.20	127.76	91.86	108.96	120.95
Total CPU	37	41	4	5	6	4	5

Maximum Per-Node, Per-CPU, CPU Temperature Maximum for Each Rack (within $72 < \text{Temp} < 150$)

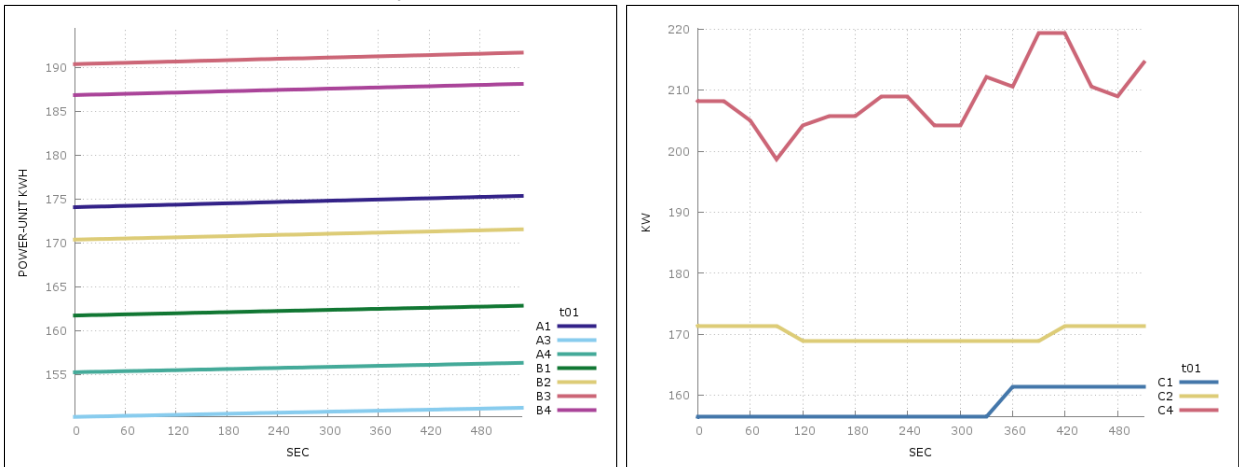
NodeAir Delta	A1	A3	A4	B1	B2	B3	B4
t01	26.80	26.20	26.62	24.52	25.28	24.37	26.24
t02	27.43	26.06	26.44	24.76	25.28	24.43	26.92
t03	29.16	25.87	26.66	24.16	25.30	24.38	27.17
Total NodeAir	23	23	21	25	23	23	15

Average Per-Node Air Temperature Delta for Each Rack (within $0 < \Delta\text{Temp} < 40$)

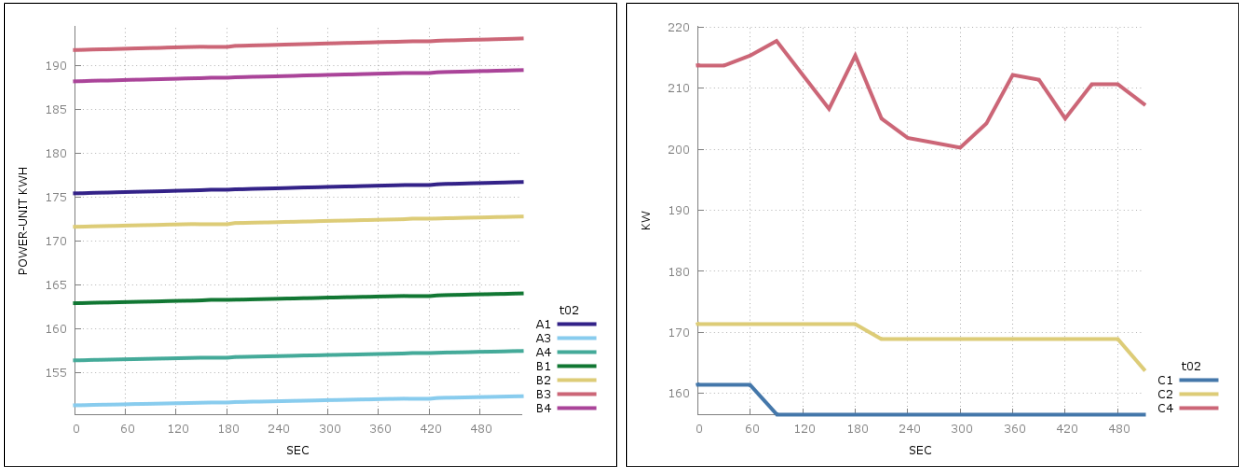
Appendix C

Low-Density Workload Chiller Metrics

Trial 1—Low-Density Workload—Power-Unit kWh Increase & Chiller KW



Trial 2—Low-Density Workload—Power-Unit kWh Increase & Chiller KW



Trial 3—Low-Density Workload—Power-Unit kWh Increase & Chiller KW

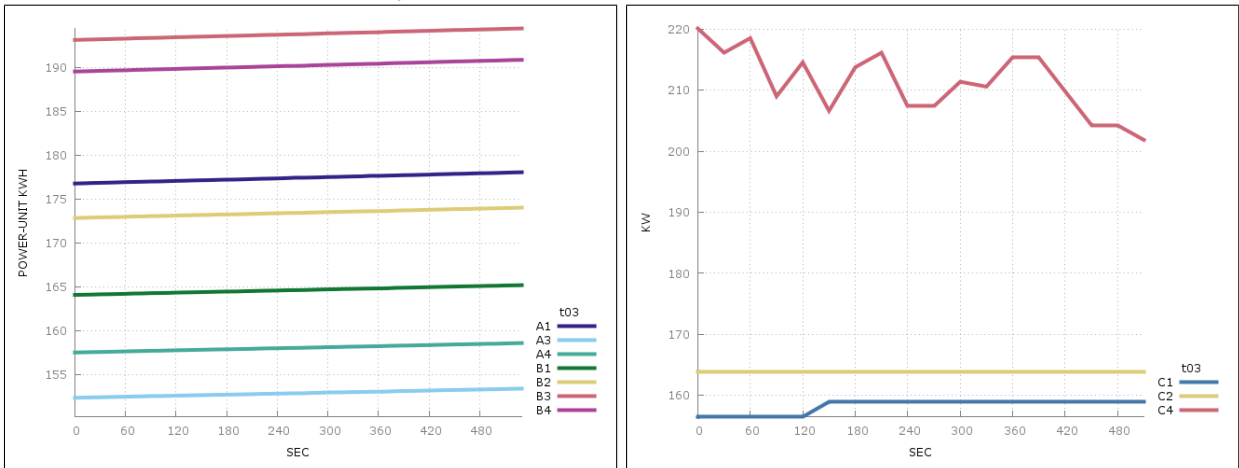
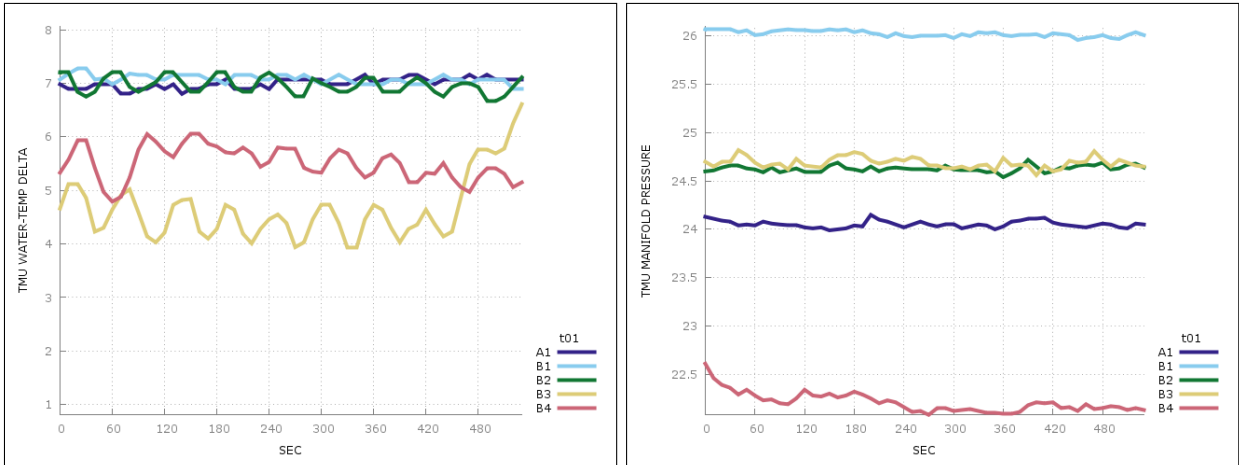
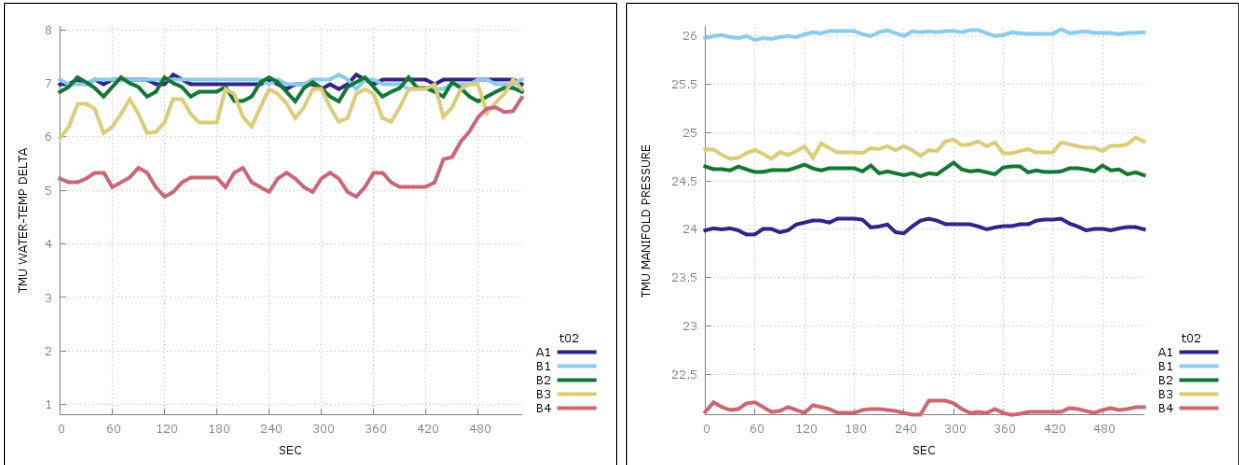


Figure C.1: The Power-Unit kWh increase (left), and the IT cooling load specified in kilowatts (left) for the Chillers in use.

Trial 1—Low-Density Workload—TMU Utilization



Trial 2—Low-Density Workload—TMU Utilization



Trial 3—Low-Density Workload—TMU Utilization

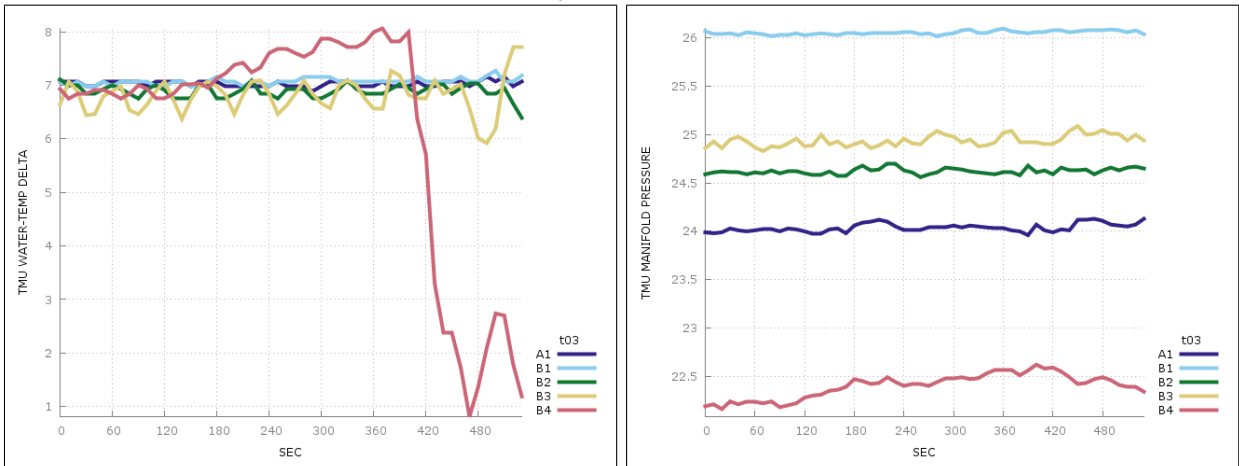
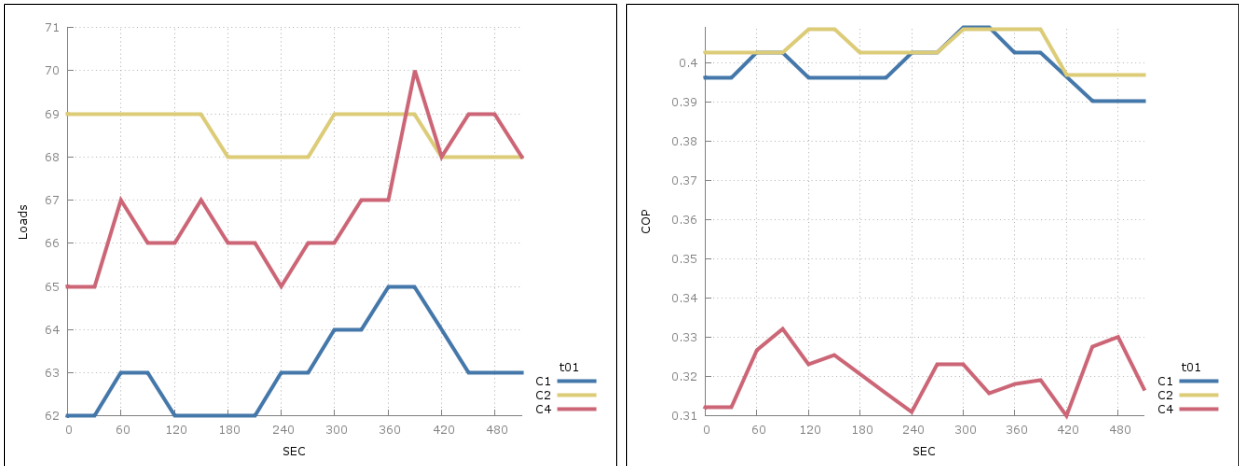
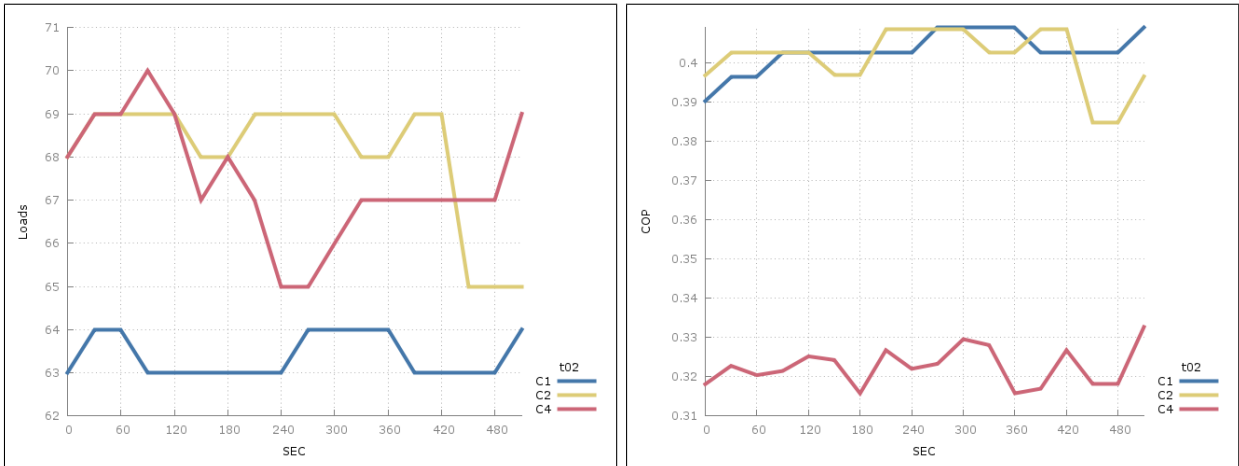


Figure C.2: TMU utilization. The water temperature delta (WTD), which is obtained by subtracting inlet from outlet temperatures, and the pressure of the hot/cold liquid distribution manifold (right).

Trial 1—Low-Density Workload—Chiller Utilization



Trial 2—Low-Density Workload—Chiller Utilization



Trial 3—Low-Density Workload—Chiller Utilization

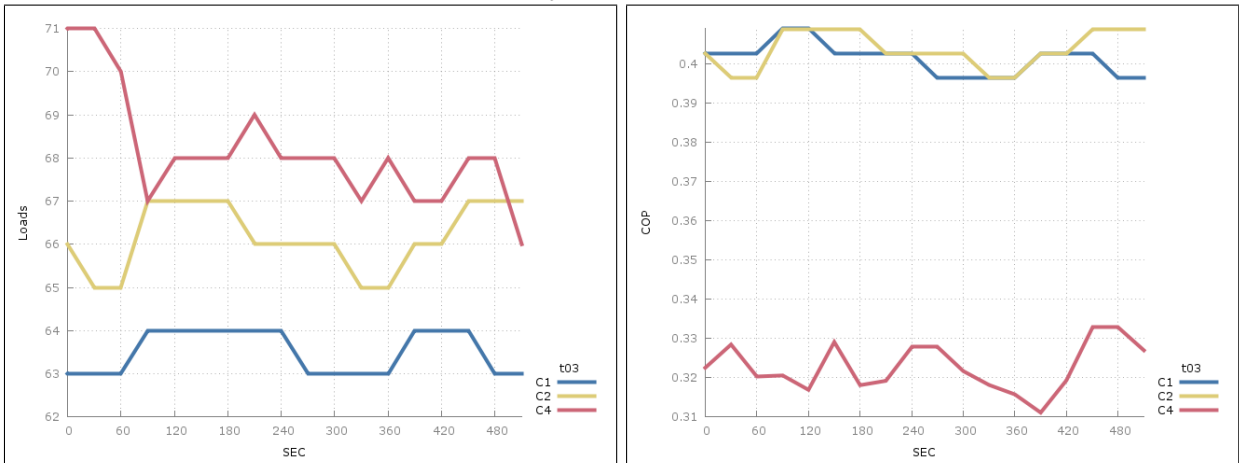
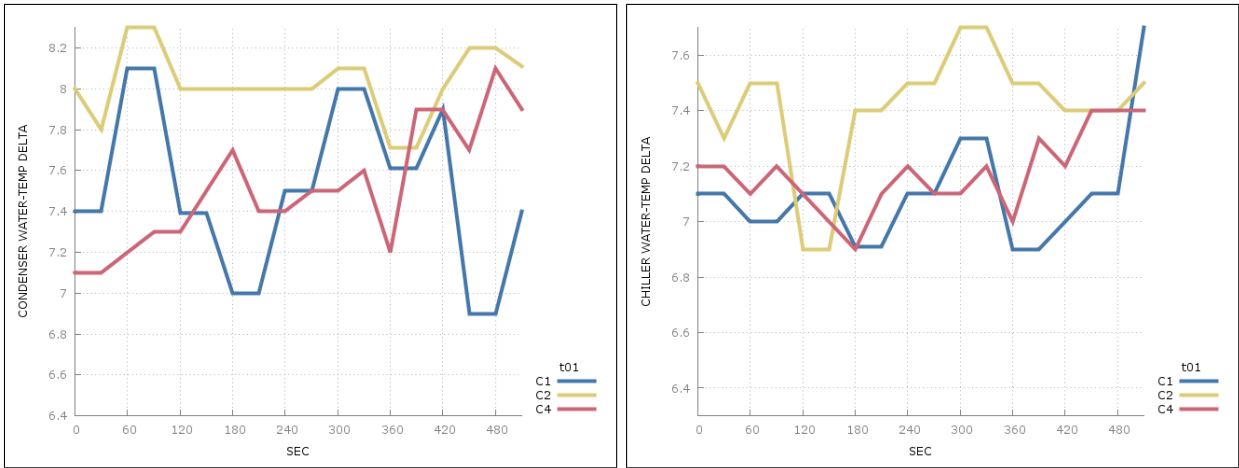
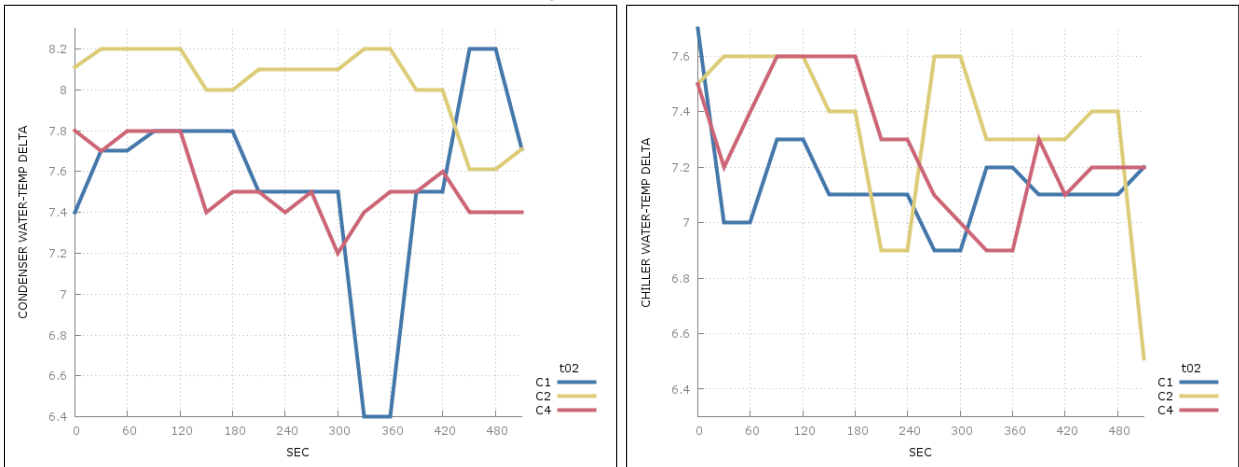


Figure C.3: Chiller Loads (left) and Chiller coefficient of performance (COP, right).

Trial 1—Low-Density Workload—Chiller Utilization



Trial 2—Low-Density Workload—Chiller Utilization



Trial 3—Low-Density Workload—Chiller Utilization

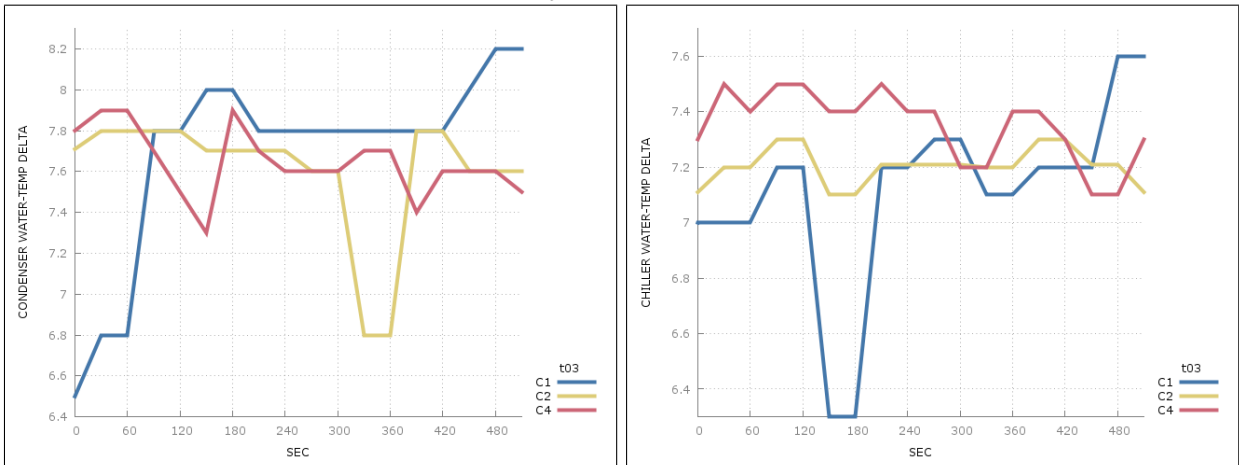
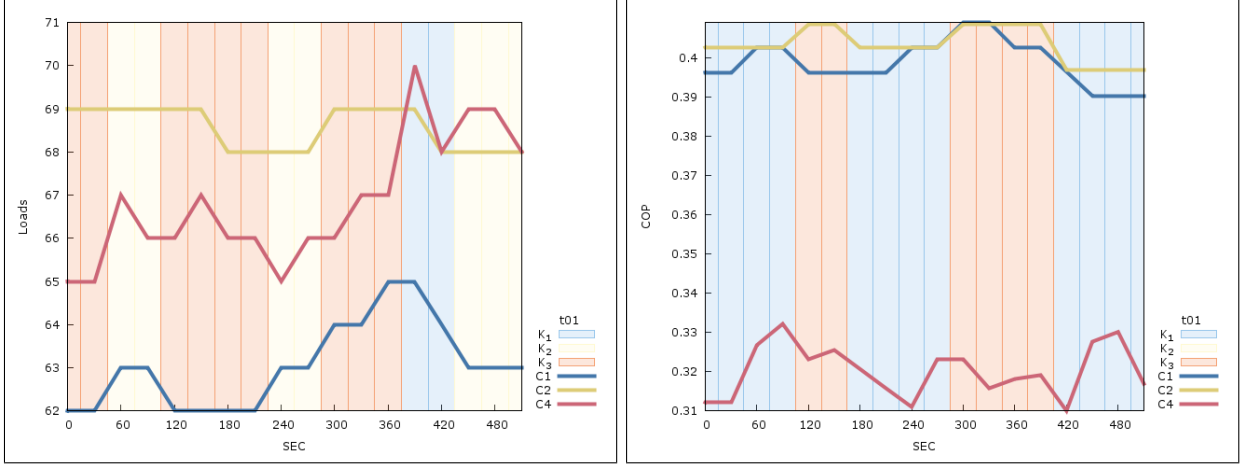


Figure C.4: Chiller utilization. The condenser water-temperature delta ($LCWT - ECWT$, left), and the Chiller water-temperature delta ($ECHWT - LCHWT$, right).

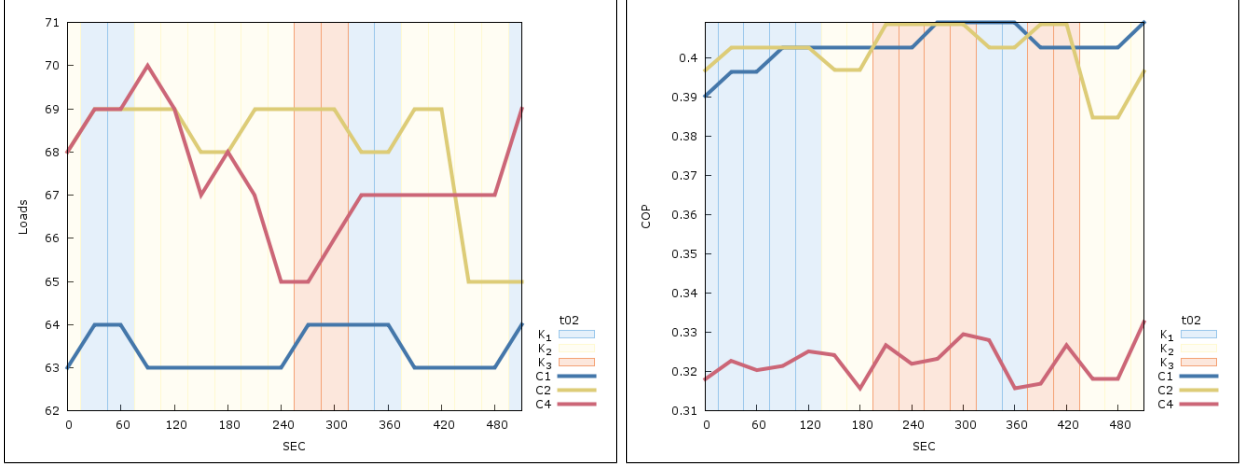
Appendix D

Clustering on Low-Density Workload Chiller Metrics

Trial 1—Low-Density Workload—Chiller Clustering



Trial 2—Low-Density Workload—Chiller Clustering



Trial 3—Low-Density Workload—Chiller Clustering

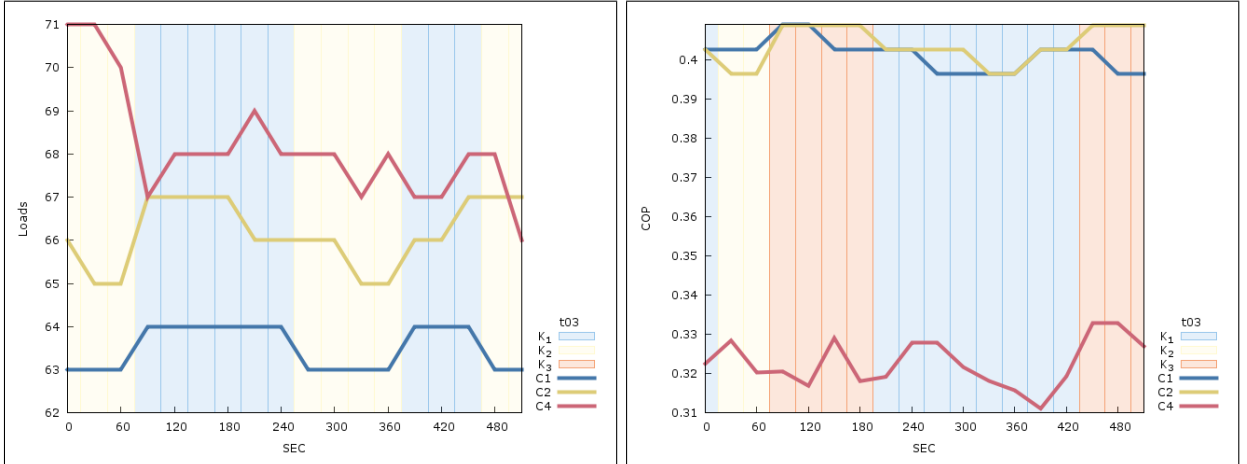
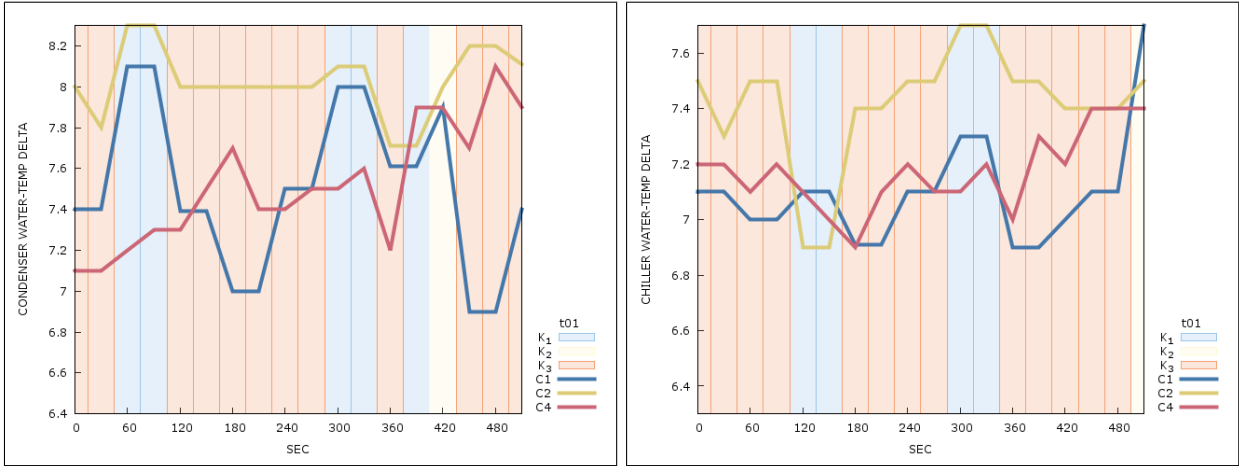
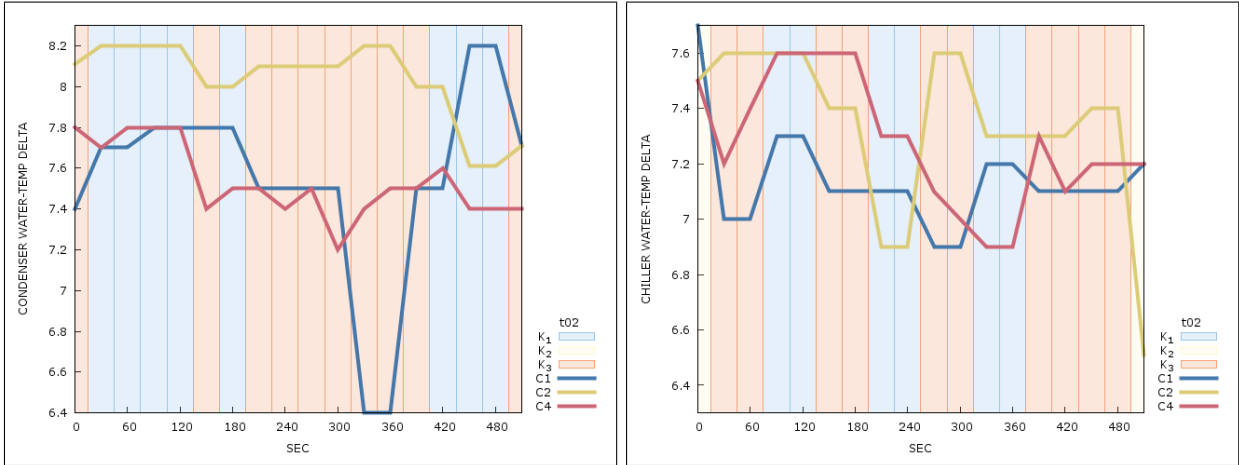


Figure D.1: Possible motifs found using EM clustering with $k = 3$ across all three trials. Chiller Loads (left) and Chiller coefficient of performance (COP, right).

Trial 1—Low-Density Workload—Chiller Clustering



Trial 2—Low-Density Workload—Chiller Clustering



Trial 3—Low-Density Workload—Chiller Clustering

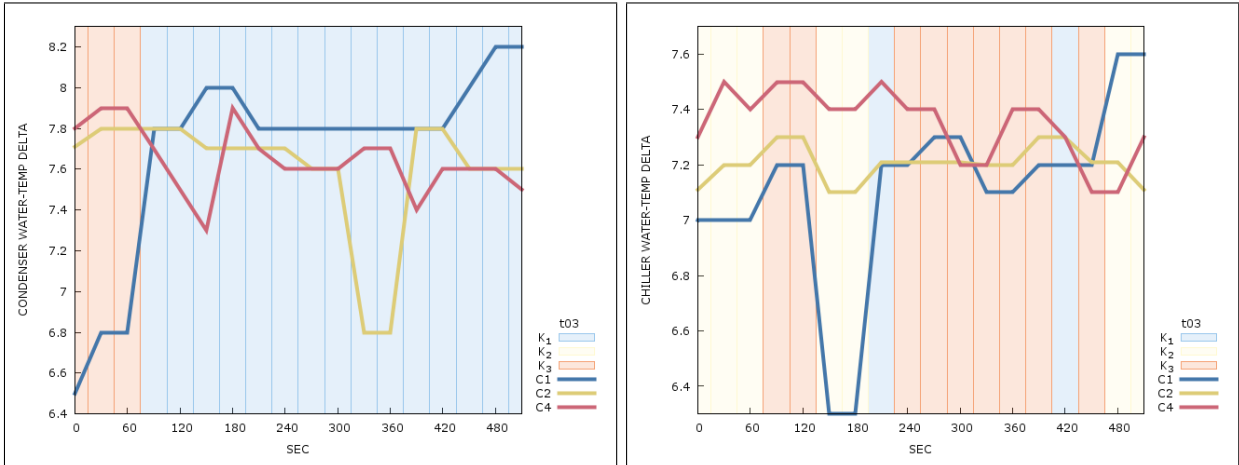


Figure D.2: Possible motifs found using EM clustering with $k = 3$ across all three trials. Chiller utilization: The condenser water-temperature delta ($LCWT - ECWT$, left), and the Chiller water-temperature delta ($ECHWT - LCHWT$, right).

Appendix E

High-Density Workload Chiller Metrics

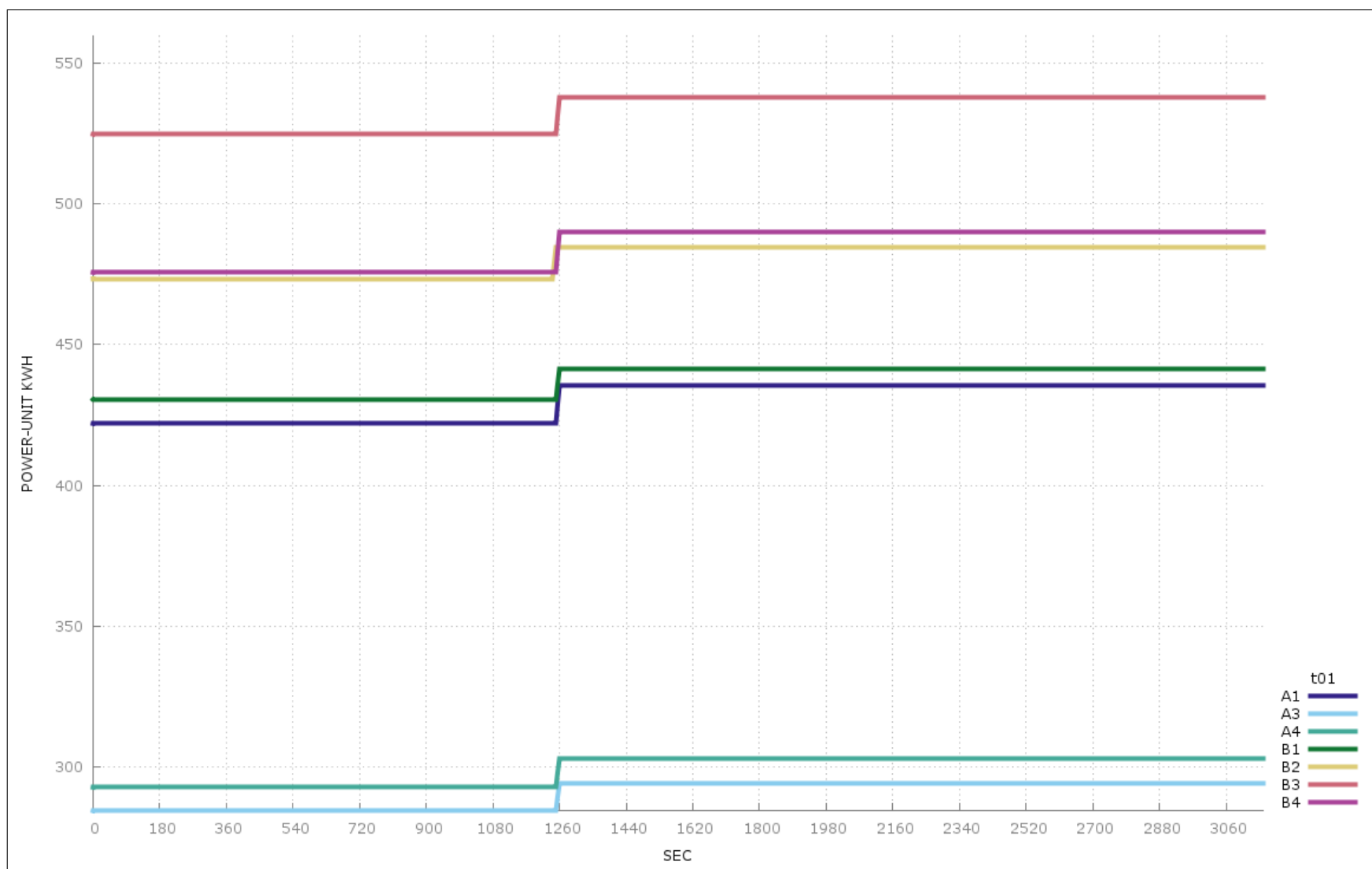


Figure E.1: Trial 1—High-Density Workload—kWh Increase

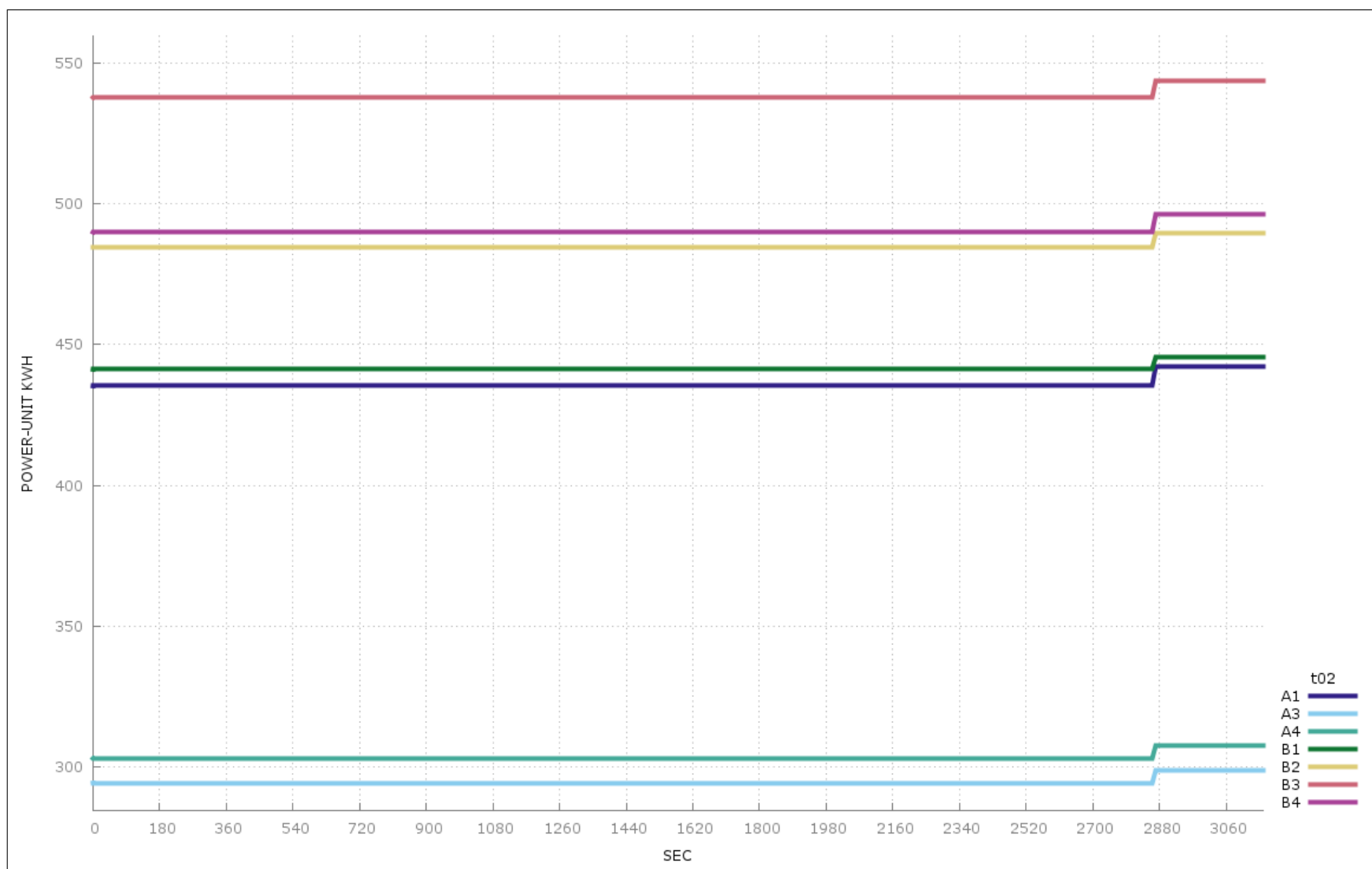


Figure E.2: Trial 2—High-Density Workload—kWh Increase

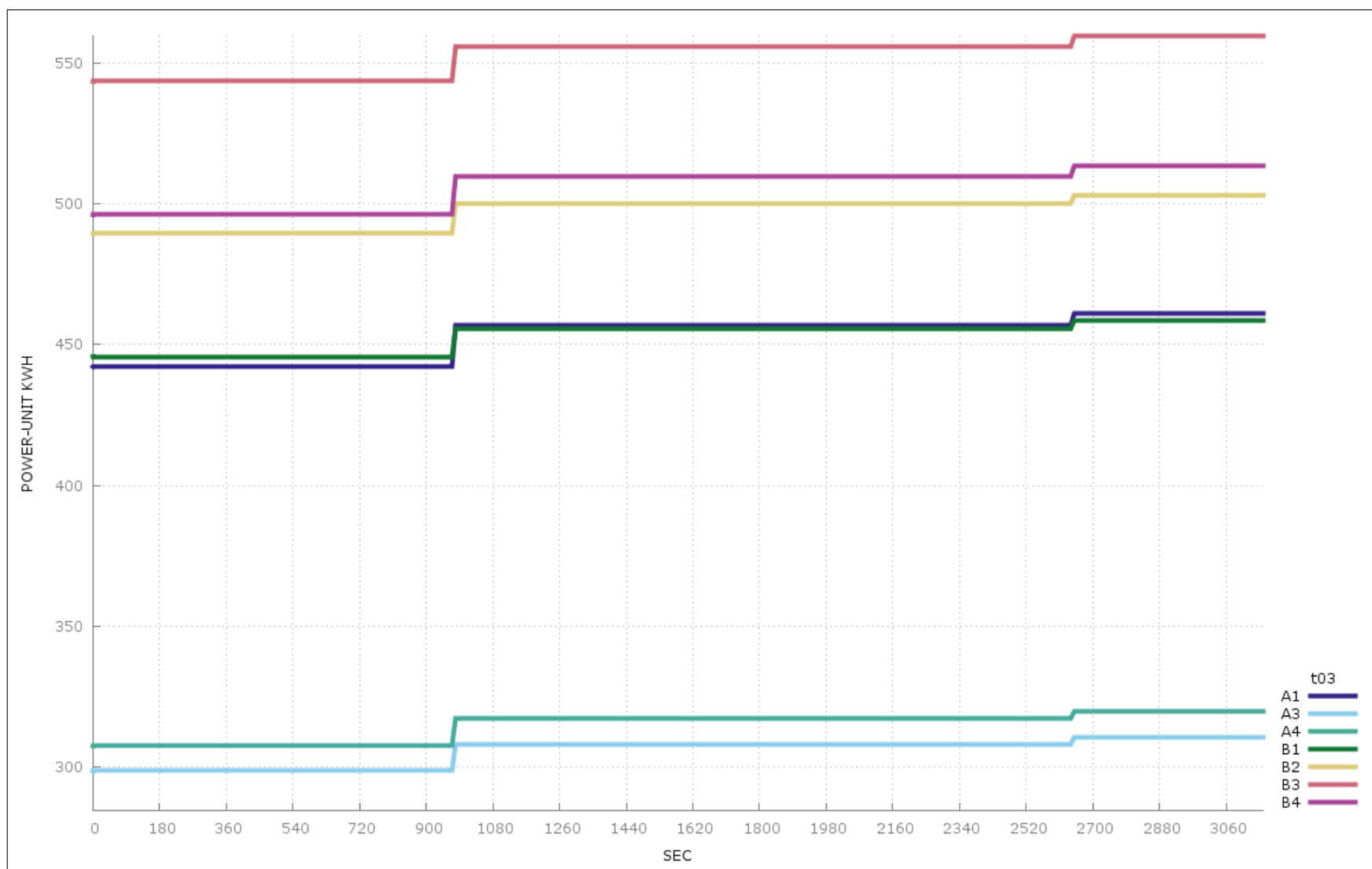


Figure E.3: Trial 3—High-Density Workload—kWh Increase

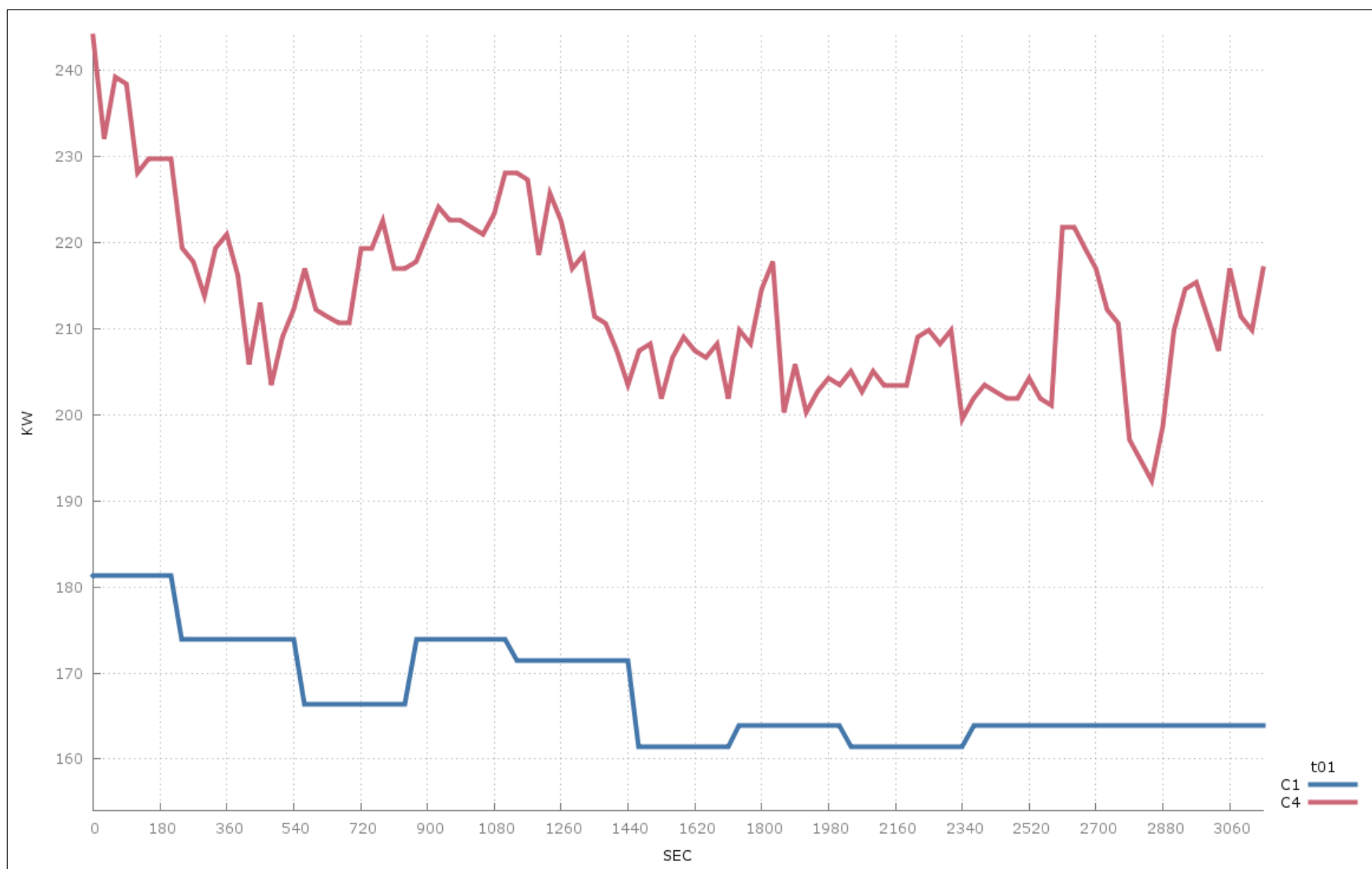


Figure E.4: Trial 1—High-Density Workload—Chiller KW

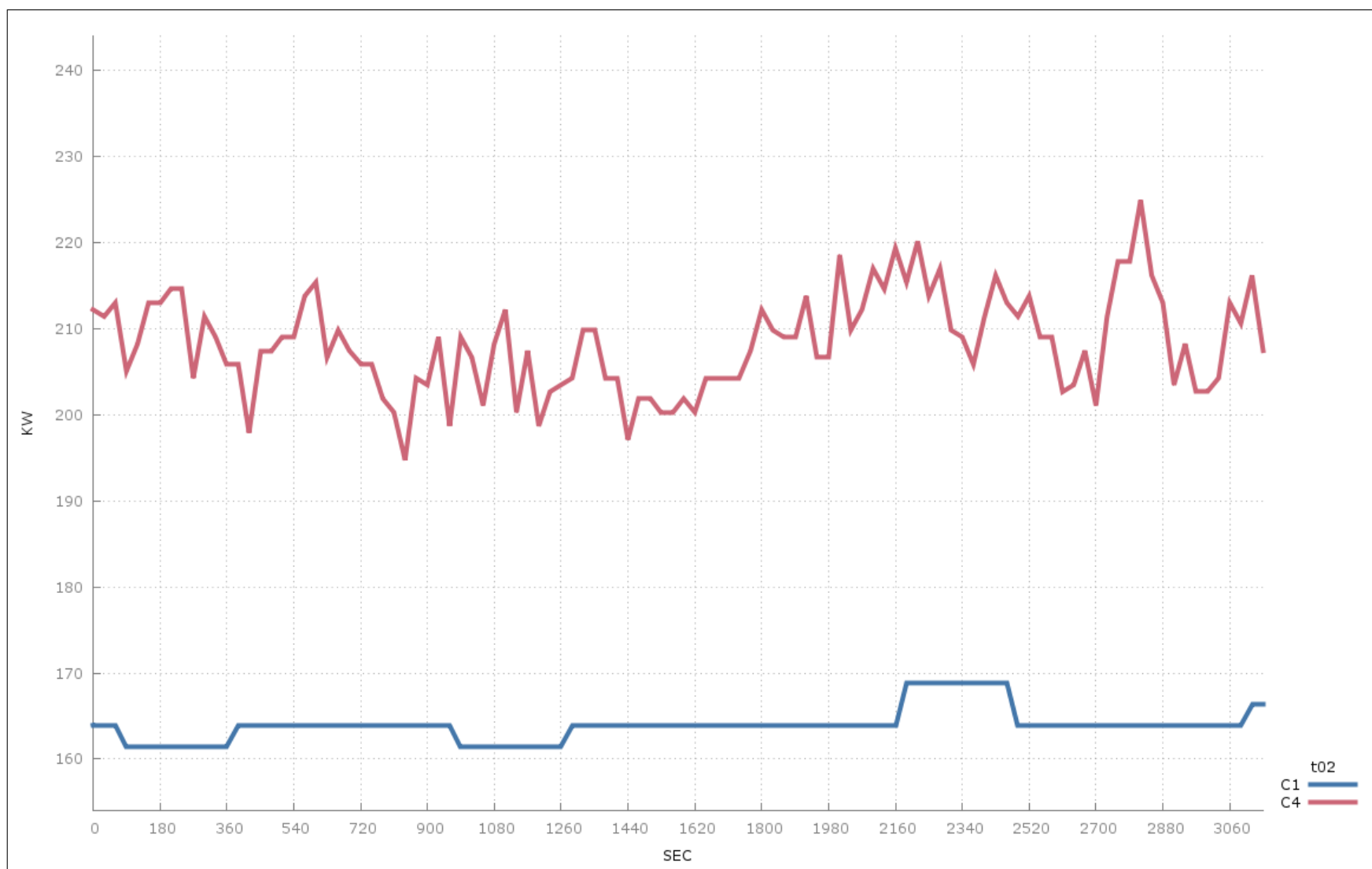


Figure E.5: Trial 2—High-Density Workload—Chiller KW

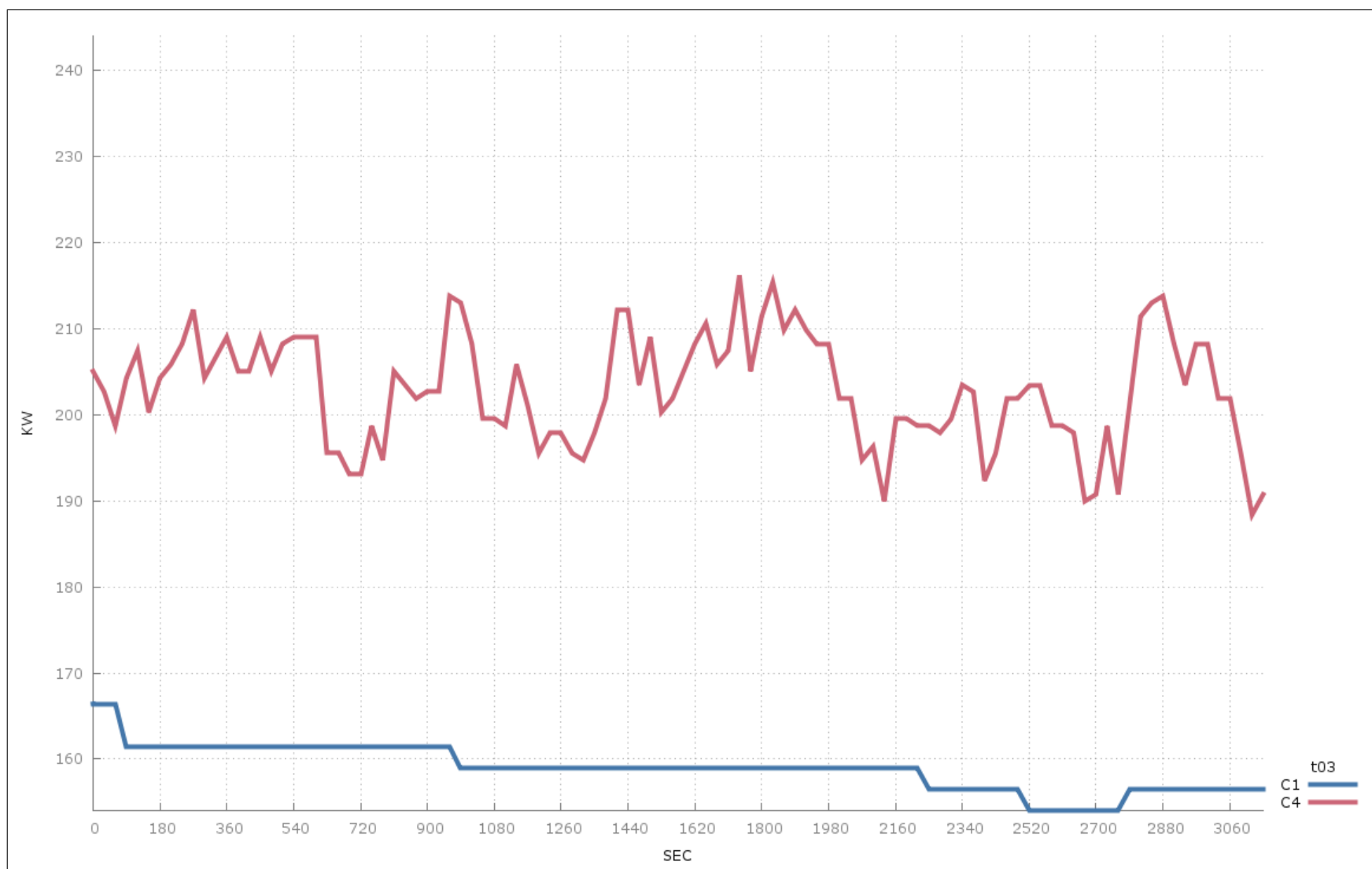


Figure E.6: Trial 3—High-Density Workload—Chiller KW

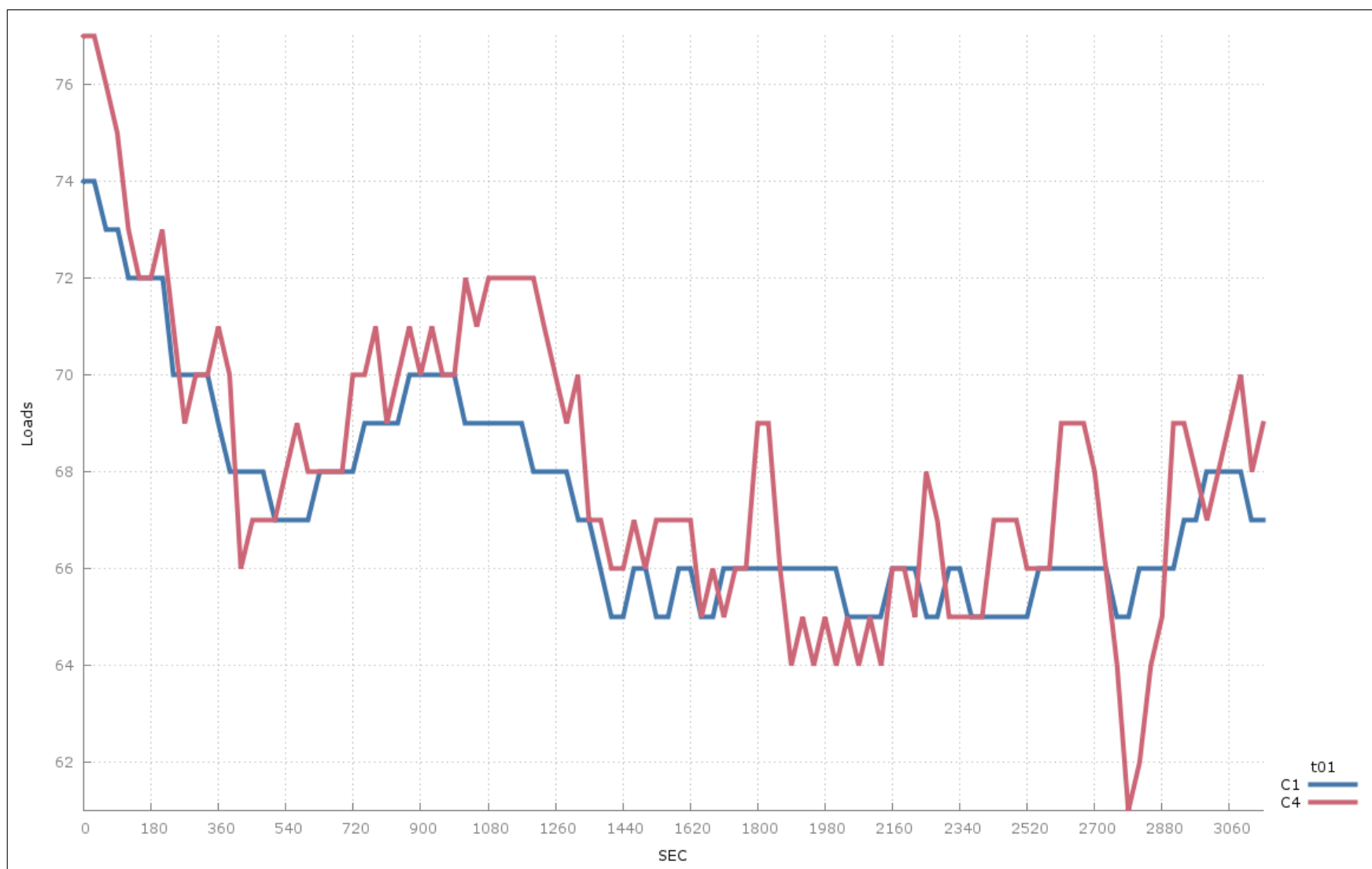


Figure E.7: Trial 1—High-Density Workload—Chiller Loads

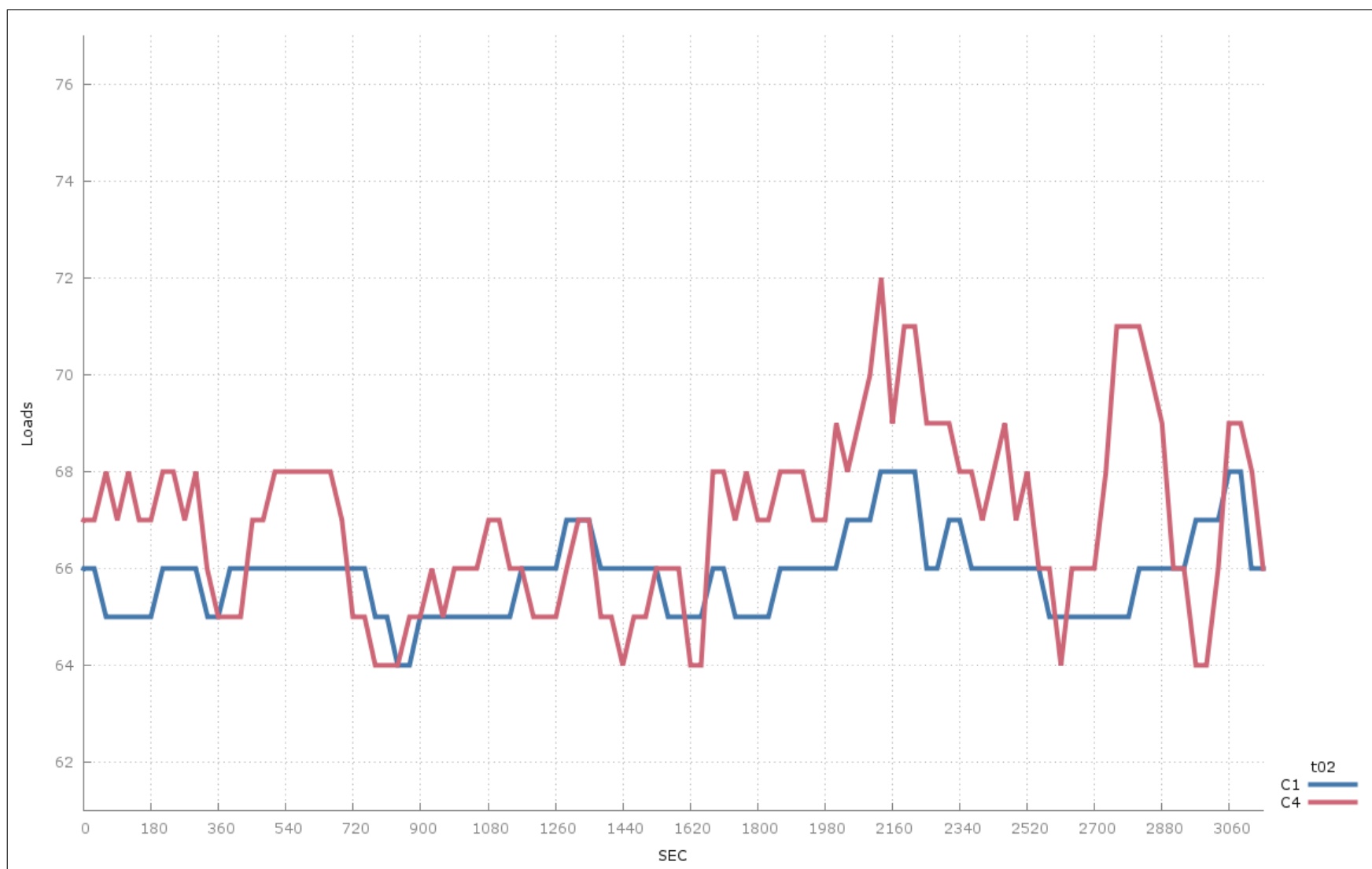


Figure E.8: Trial 2—High-Density Workload—Chiller Loads

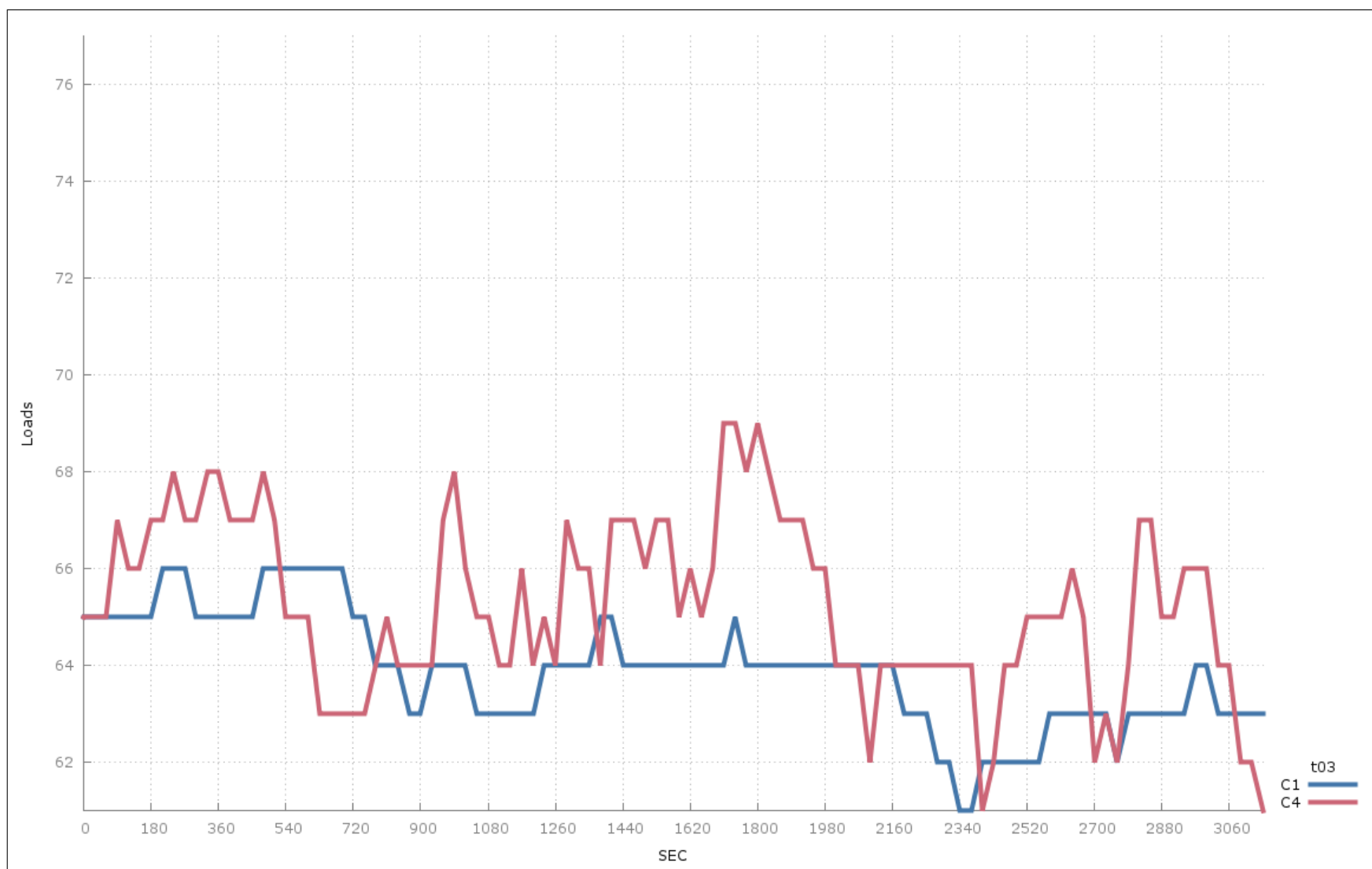


Figure E.9: Trial 3—High-Density Workload—Chiller Loads

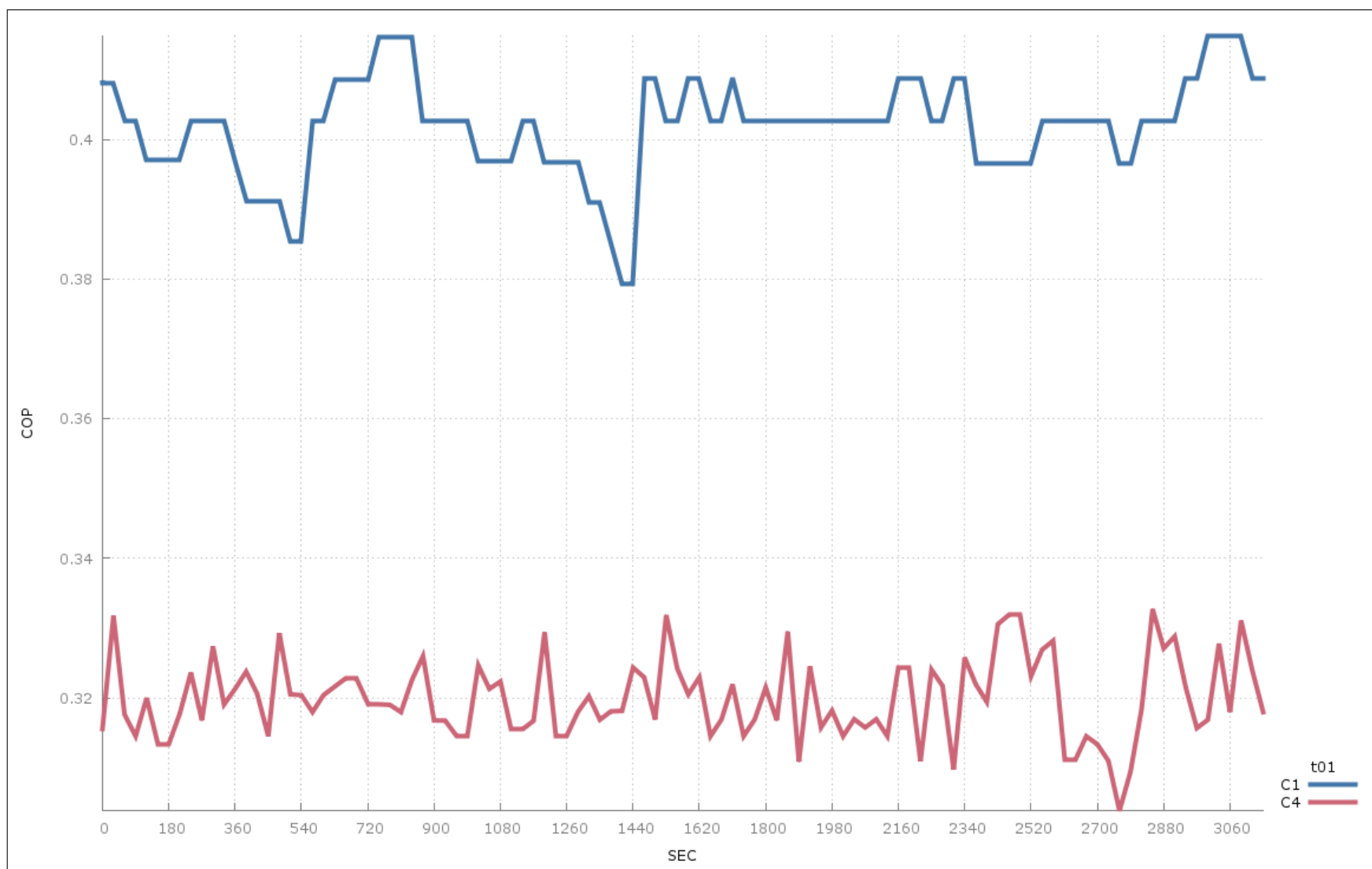


Figure E.10: Trial 1—High-Density Workload—Chiller COP

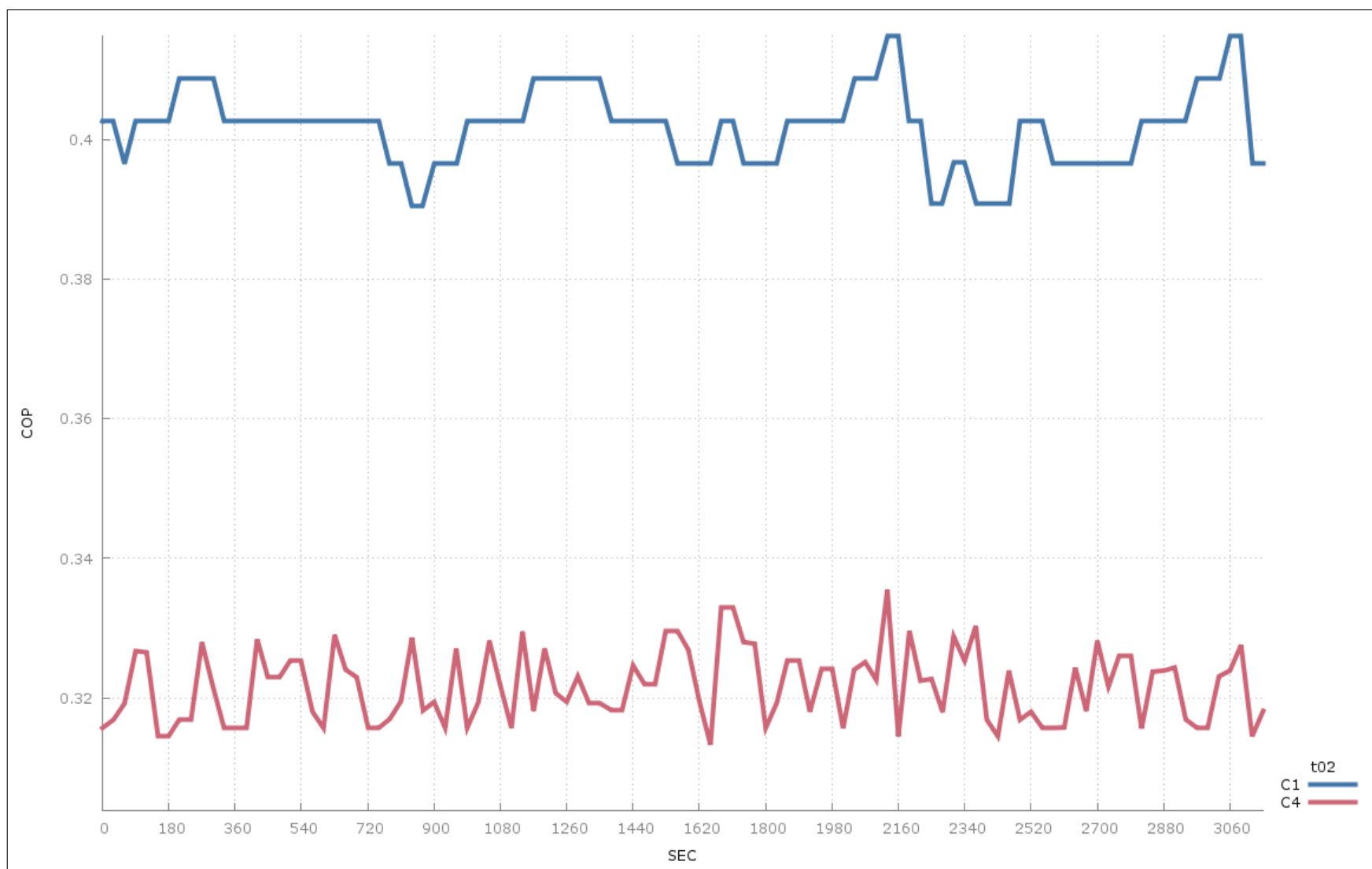


Figure E.11: Trial 2—High-Density Workload—Chiller COP

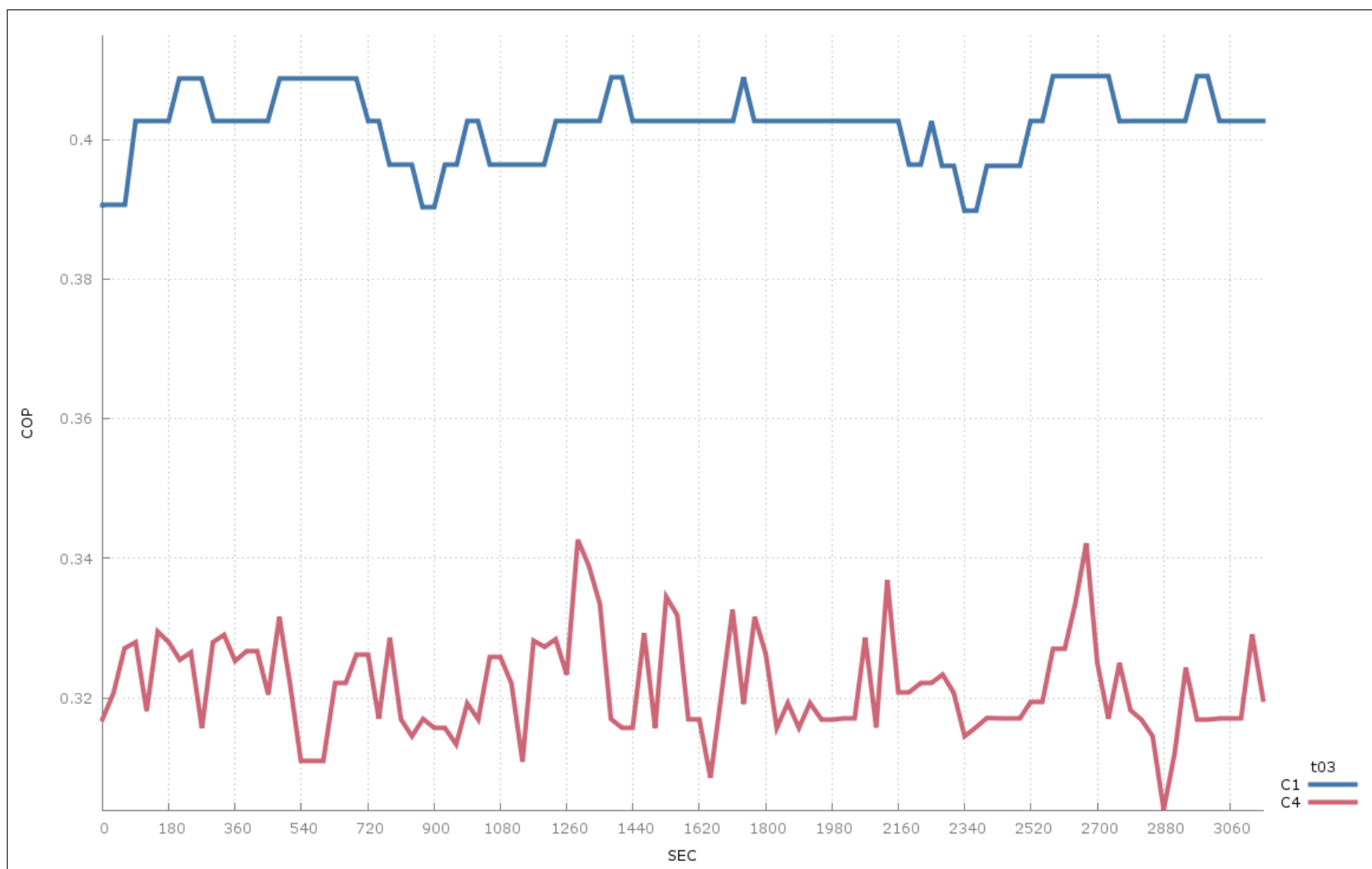


Figure E.12: Trial 3—High-Density Workload—Chiller COP

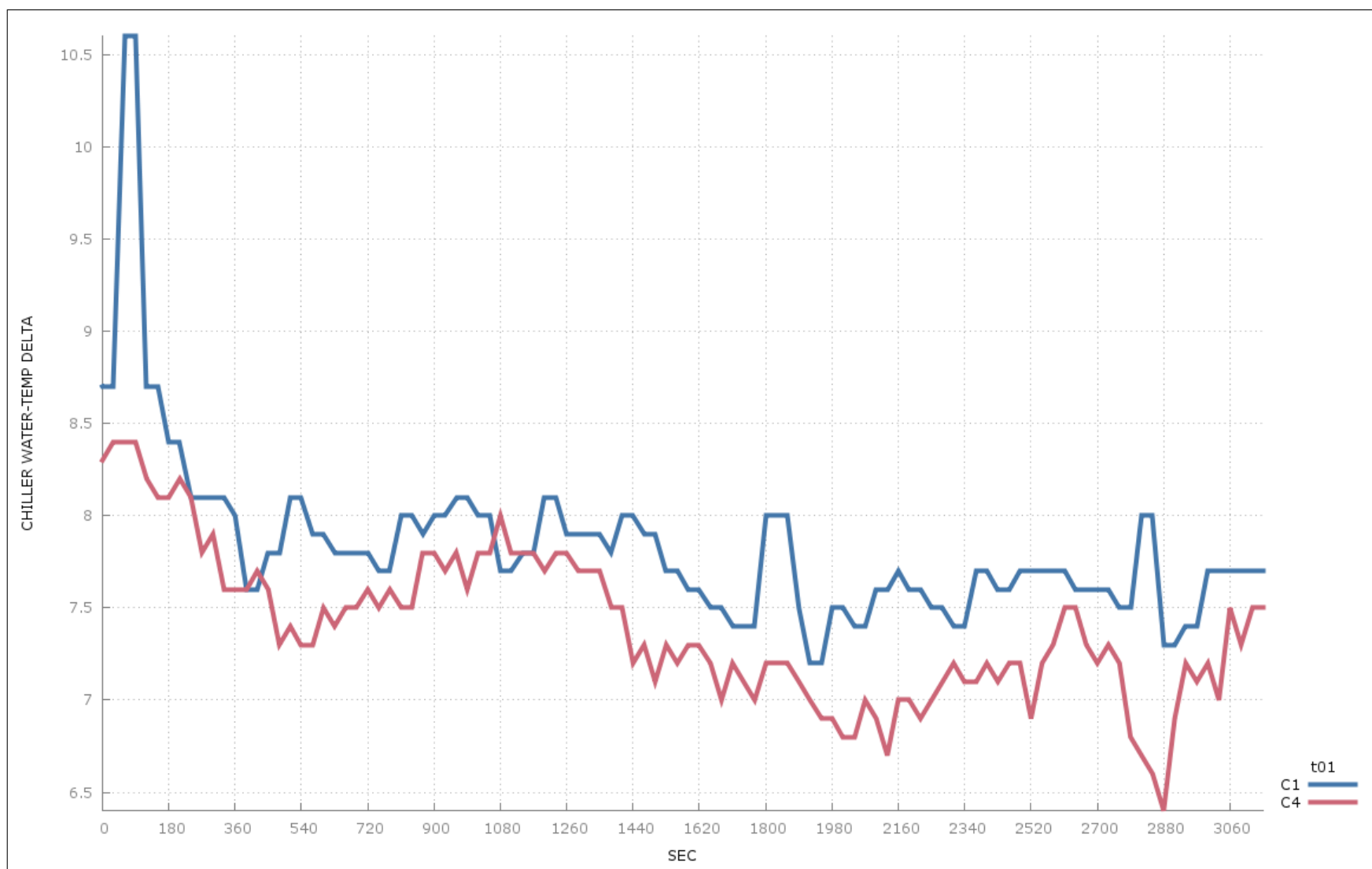


Figure E.13: Trial 1—High-Density Workload—Chiller Chilled Water Temperature Delta

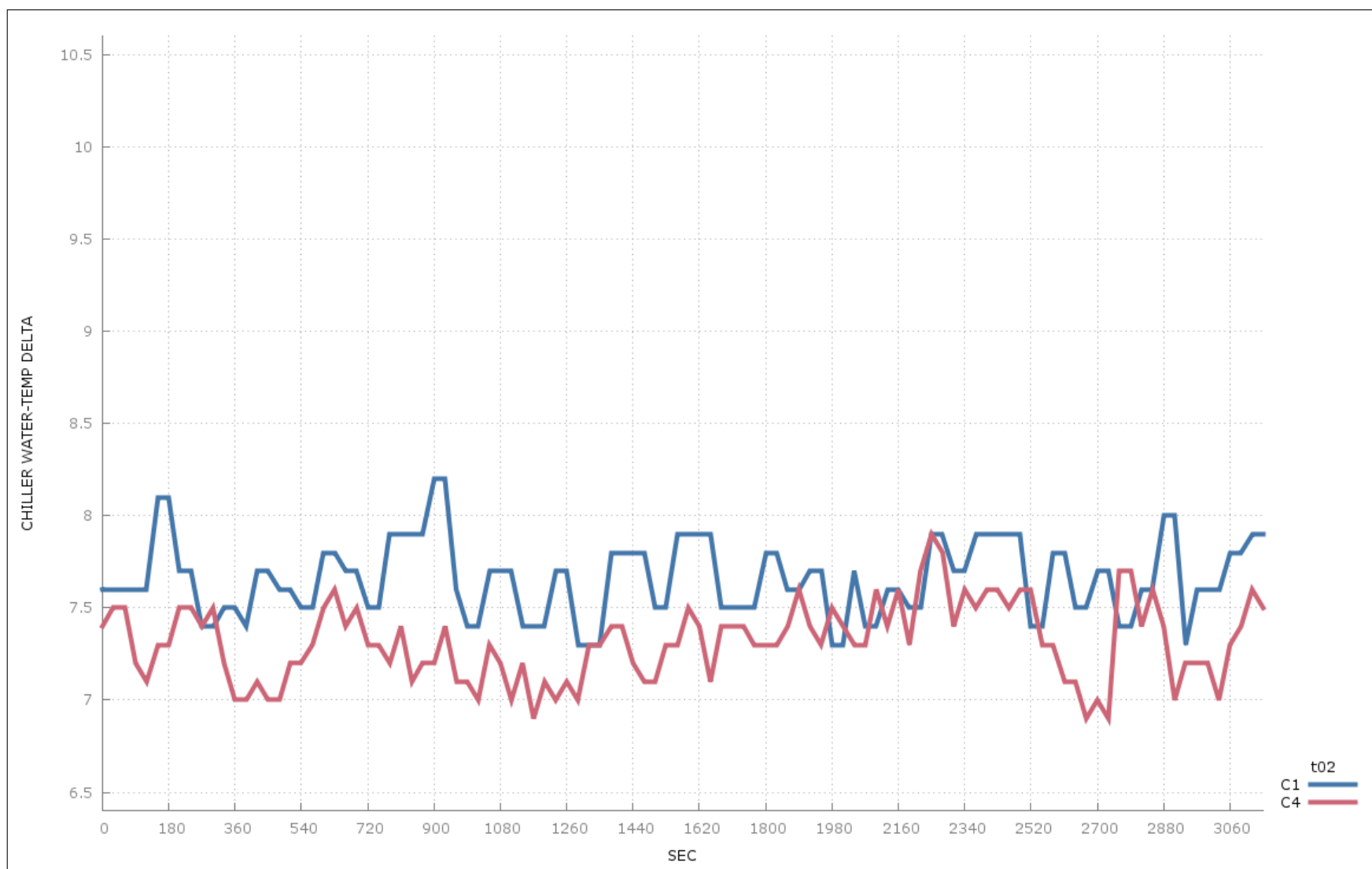


Figure E.14: Trial 2—High-Density Workload—Chiller Chilled Water Temperature Delta

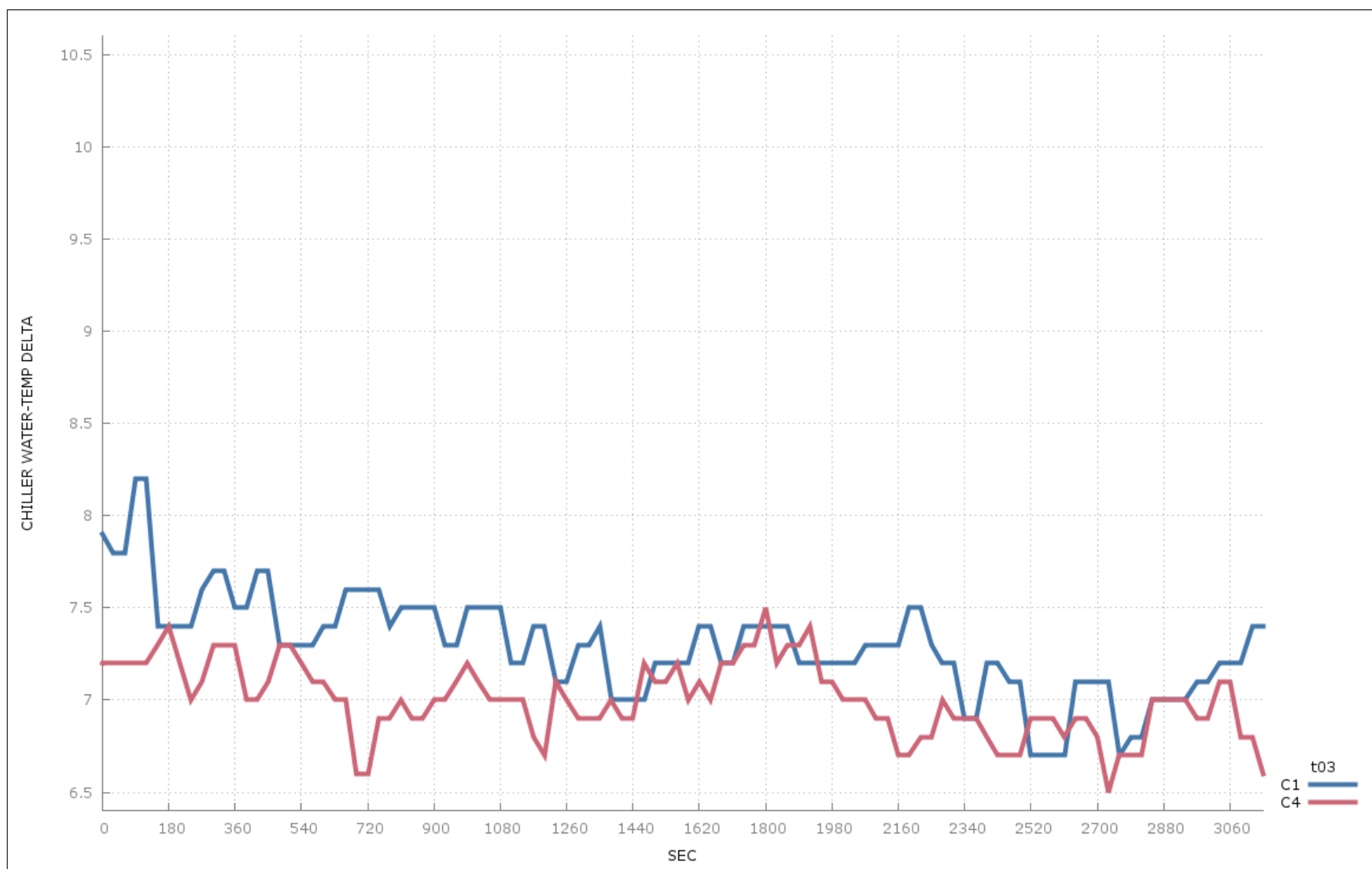


Figure E.15: Trial 3—High-Density Workload—Chiller Chilled Water Temperature Delta

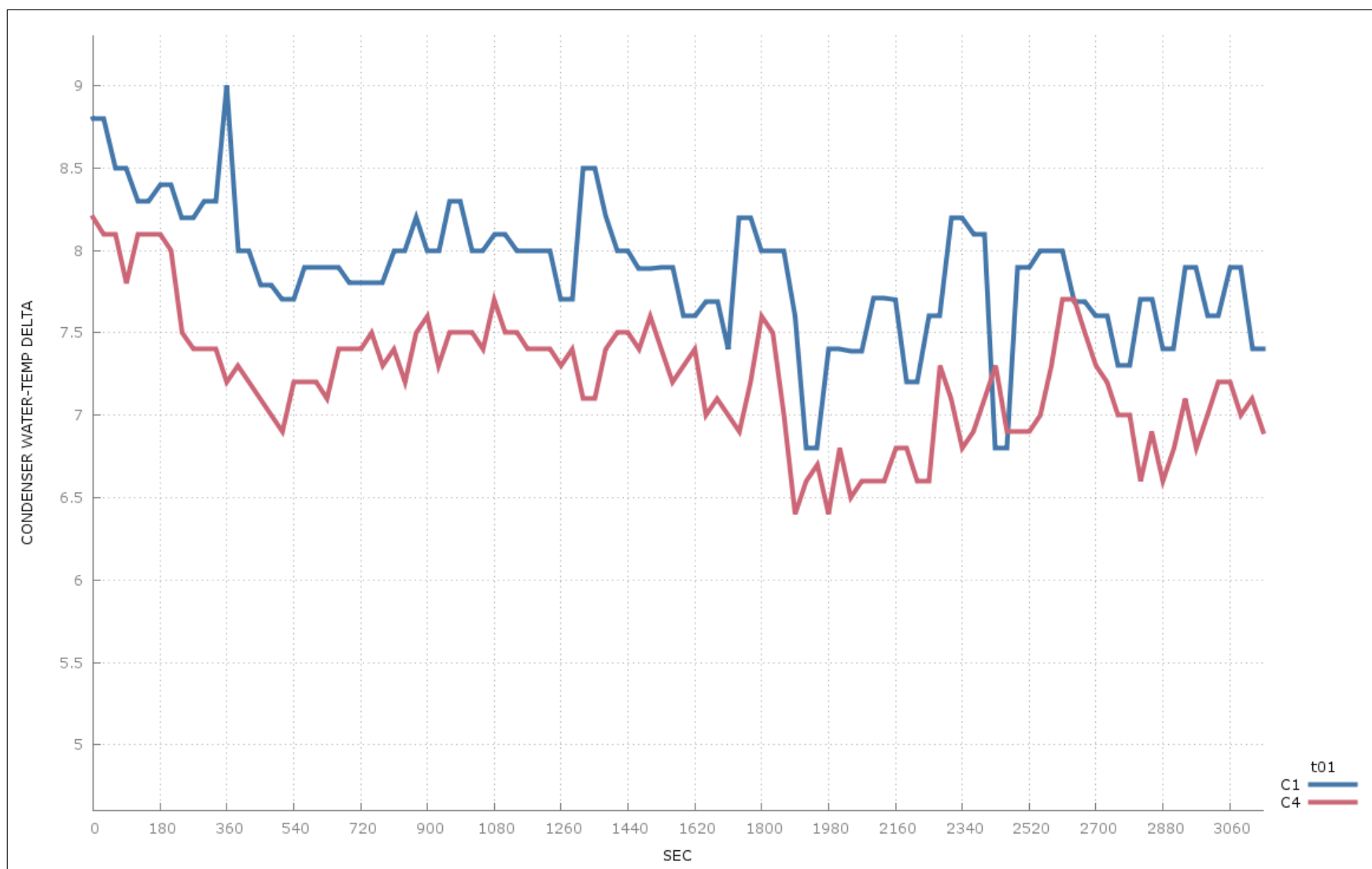


Figure E.16: Trial 1—High-Density Workload—Chiller Condenser Water Temperature Delta

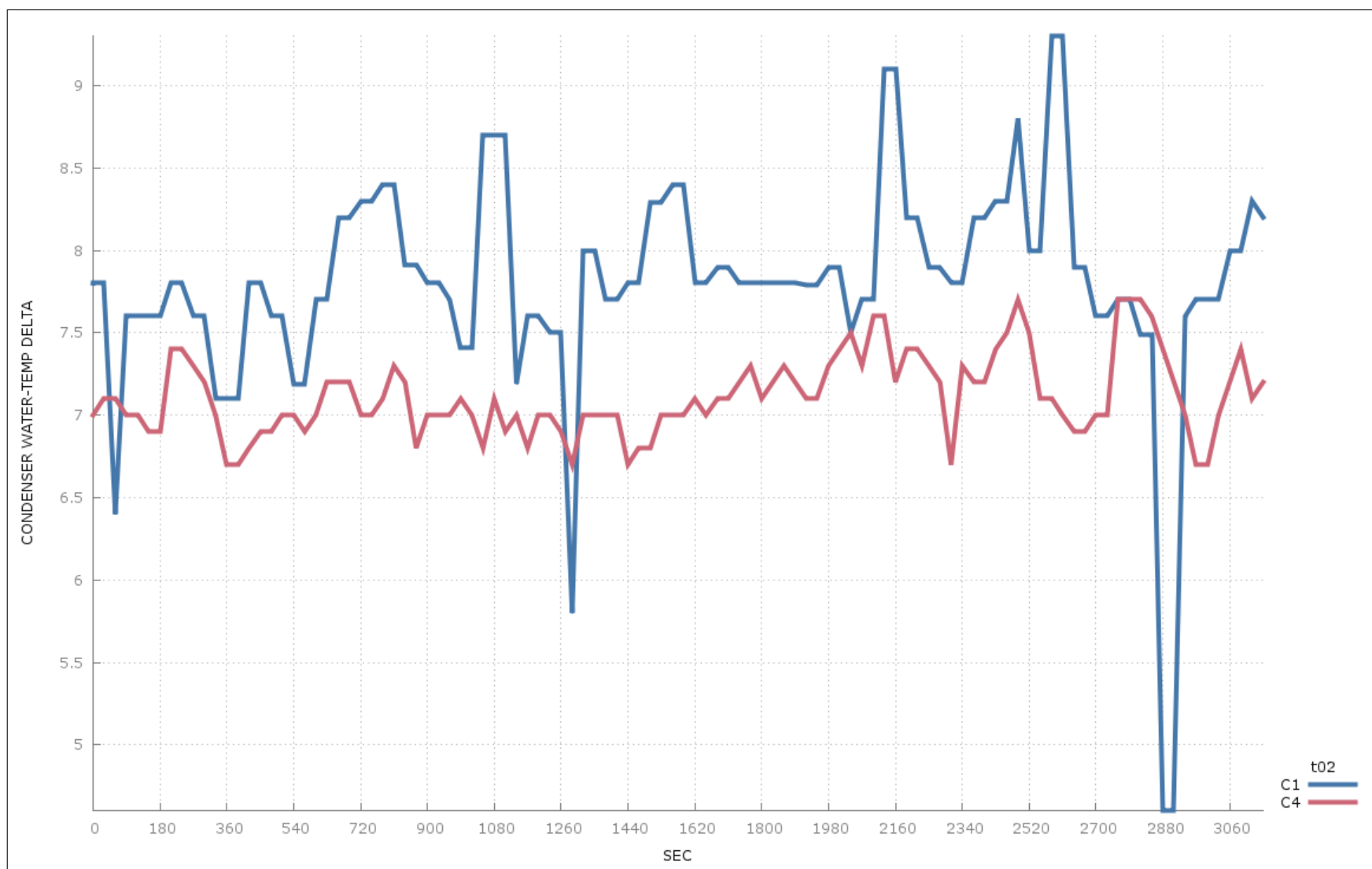


Figure E.17: Trial 2—High-Density Workload—Chiller Condenser Water Temperature Delta

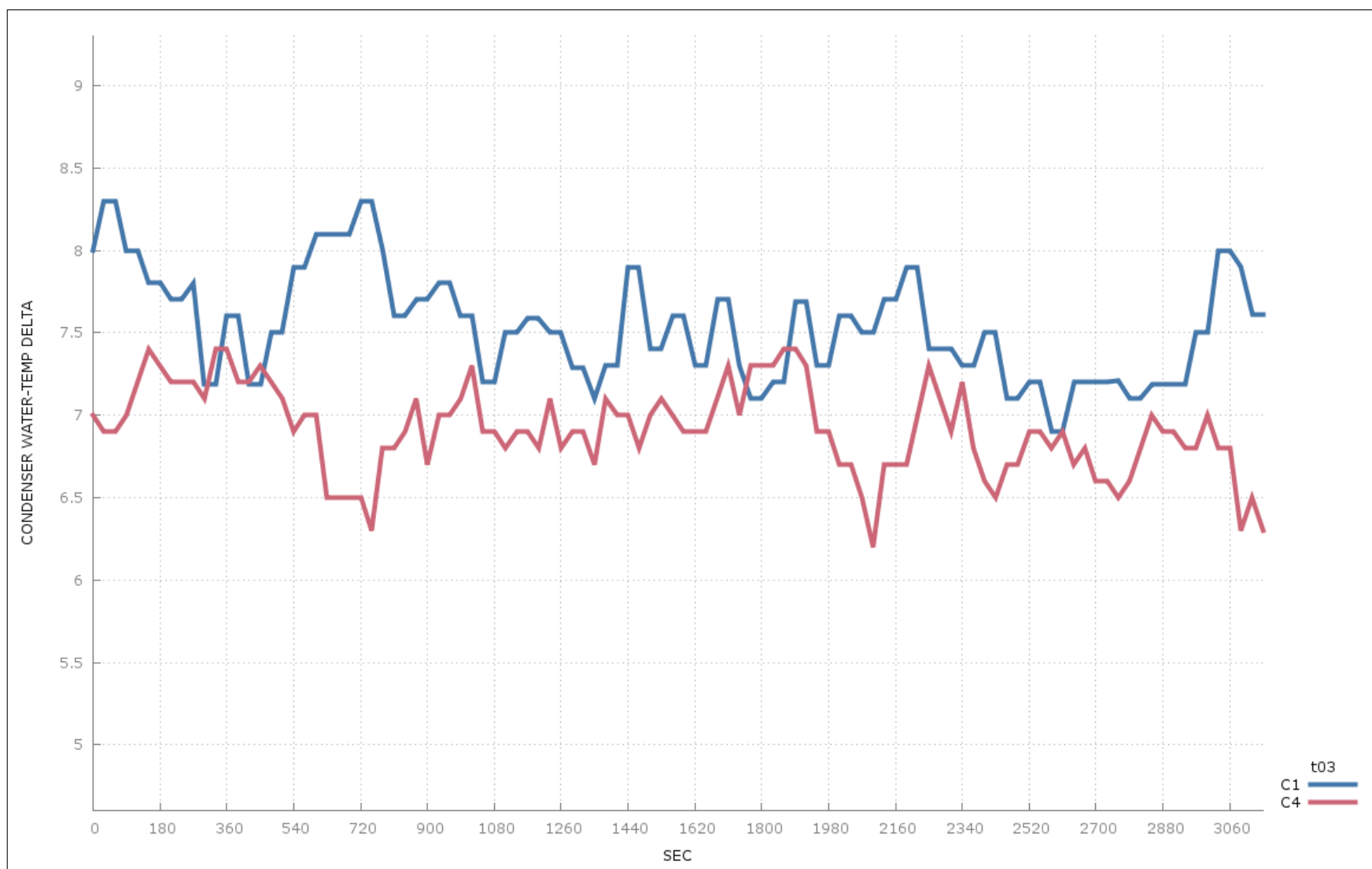


Figure E.18: Trial 3—High-Density Workload—Chiller Condenser Water Temperature Delta

Appendix F

**Clustering on High-Density Workload Chiller
Metrics (EM clustering with $k = 3$ across all three
trials)**

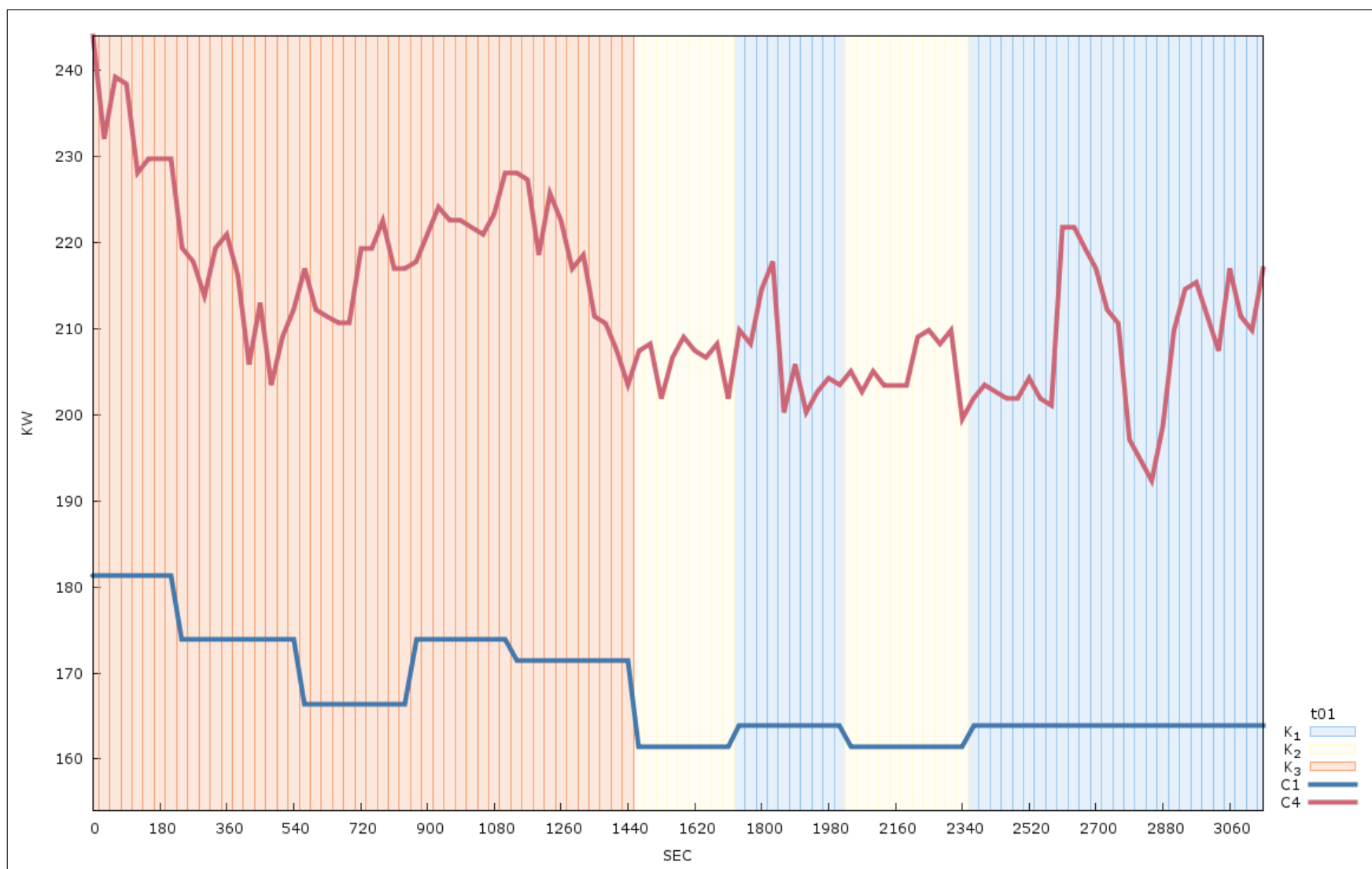


Figure F.1: Trial 1—High-Density Workload—Chiller Clustering on KW

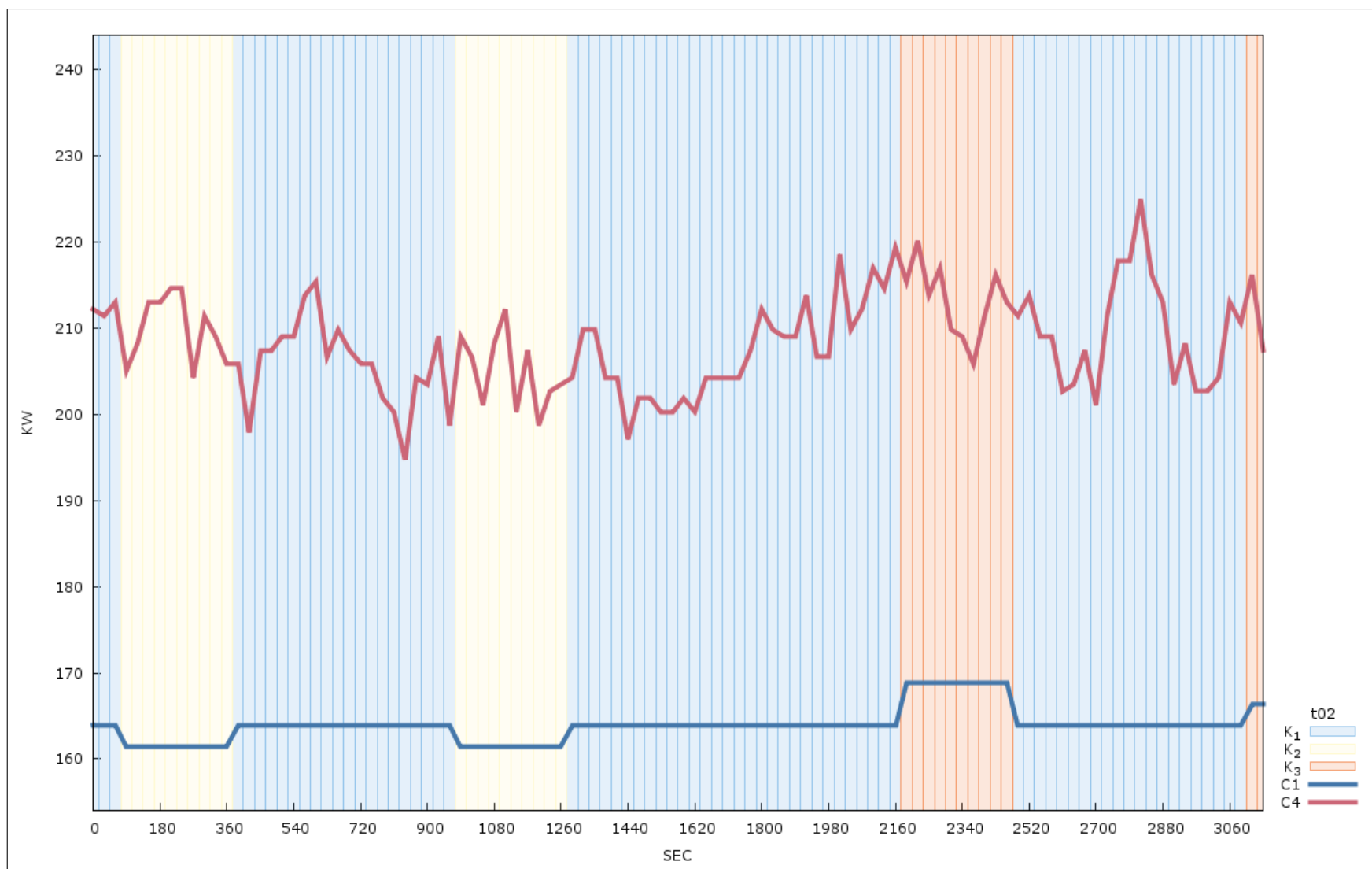


Figure F.2: Trial 2—High-Density Workload—Chiller Clustering on KW

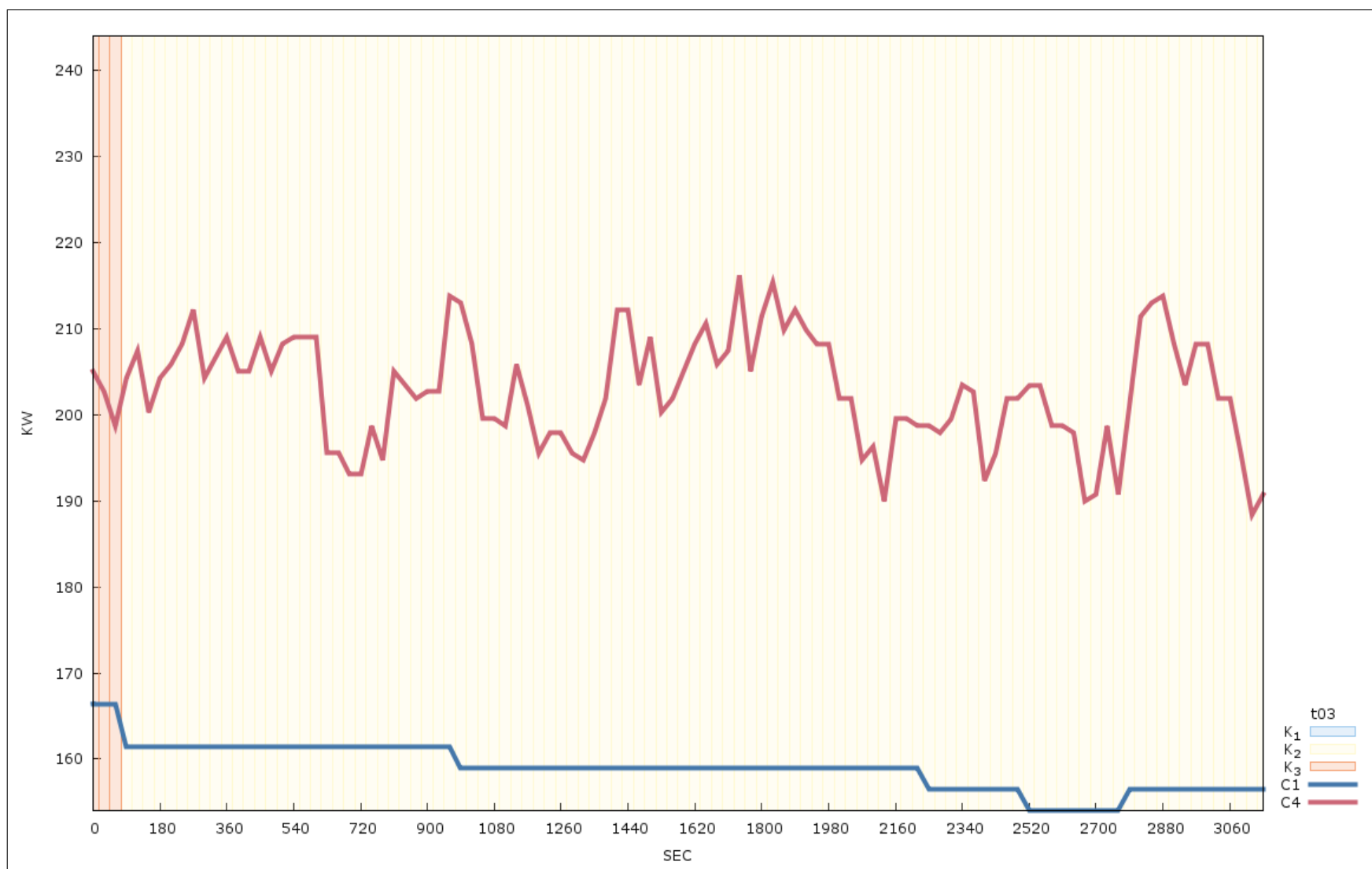


Figure F.3: Trial 3—High-Density Workload—Chiller Clustering on KW

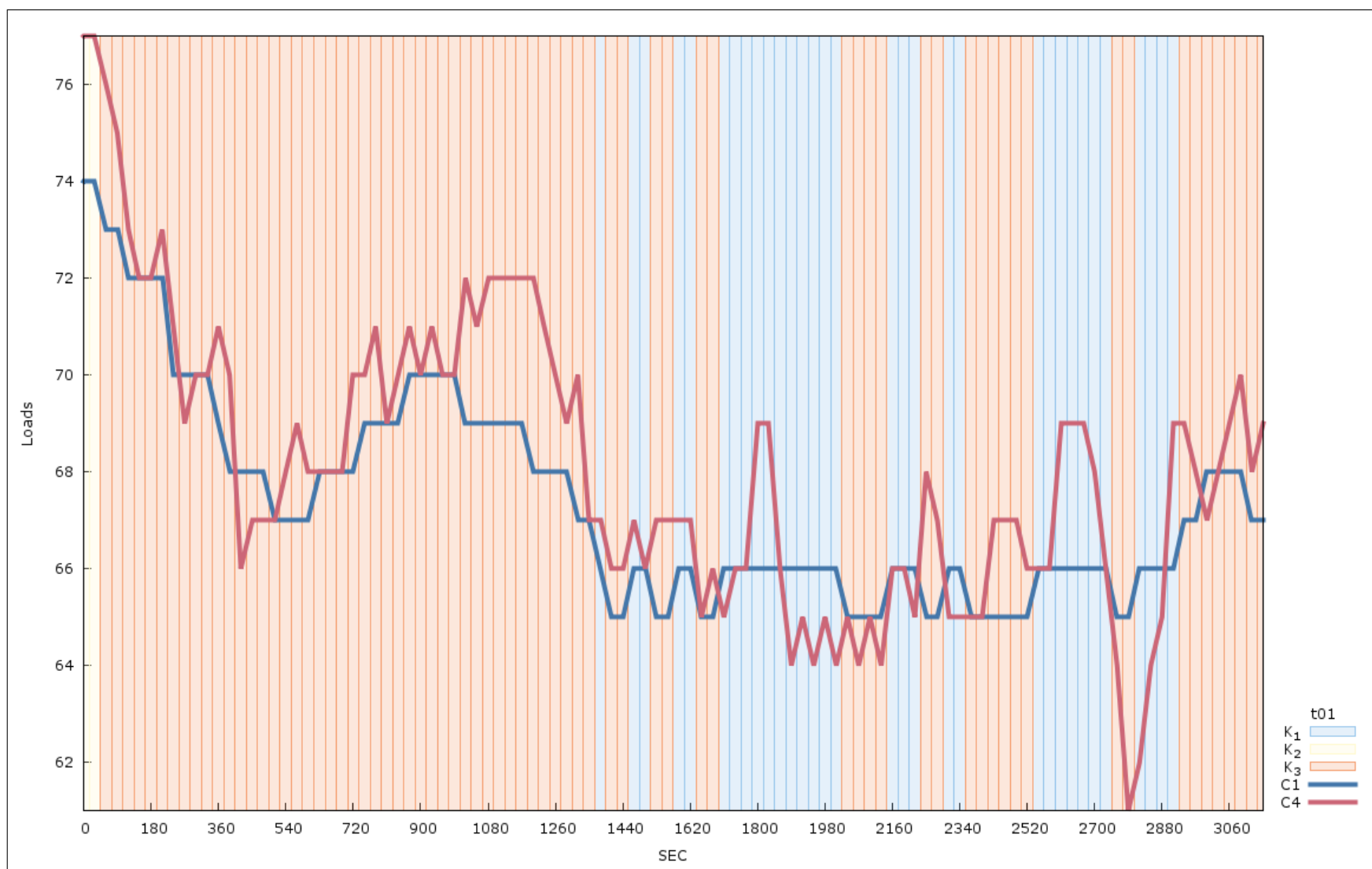


Figure F.4: Trial 1—High-Density Workload—Chiller Clustering on Loads

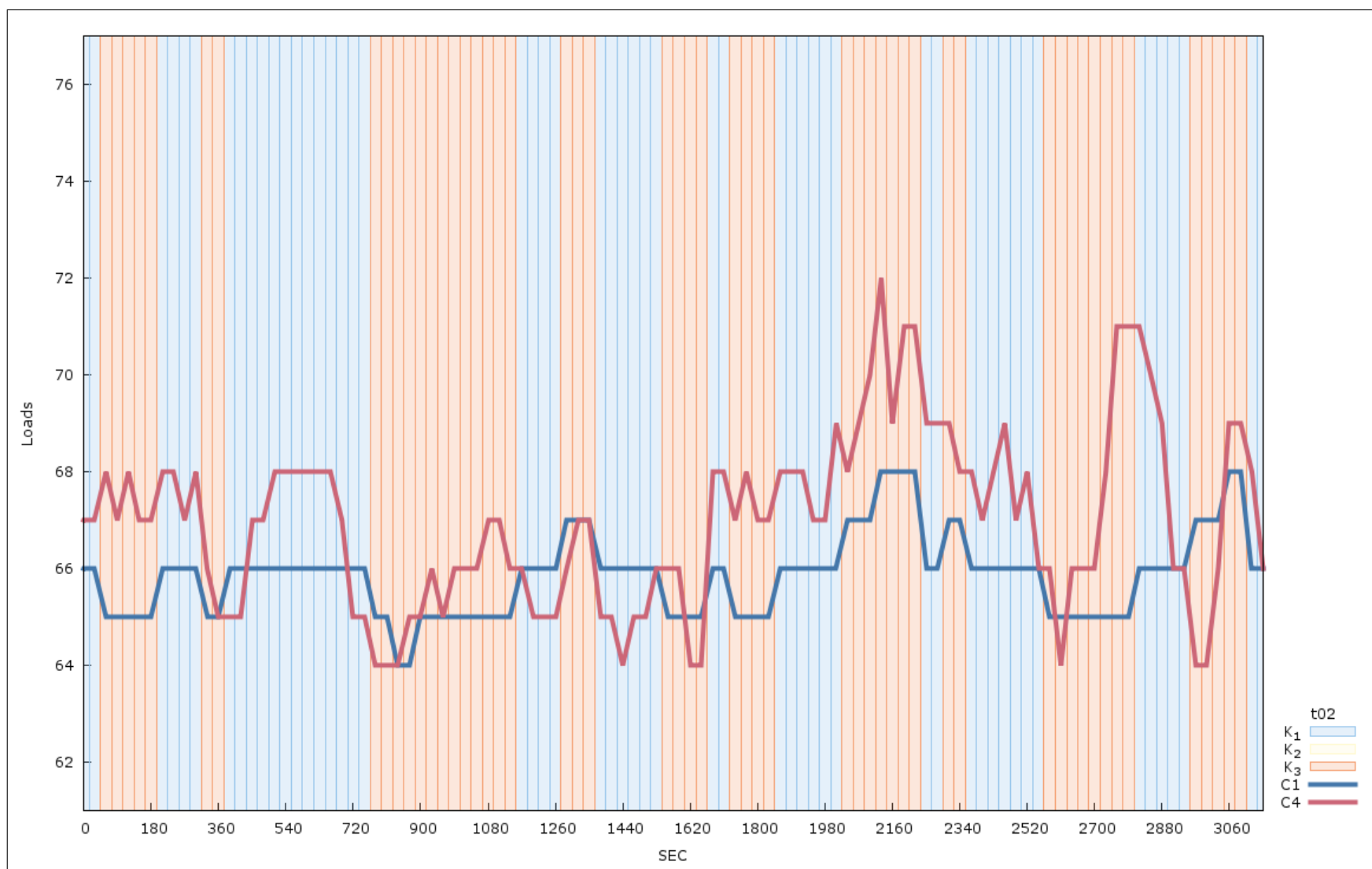


Figure F.5: Trial 2—High-Density Workload—Chiller Clustering on Loads

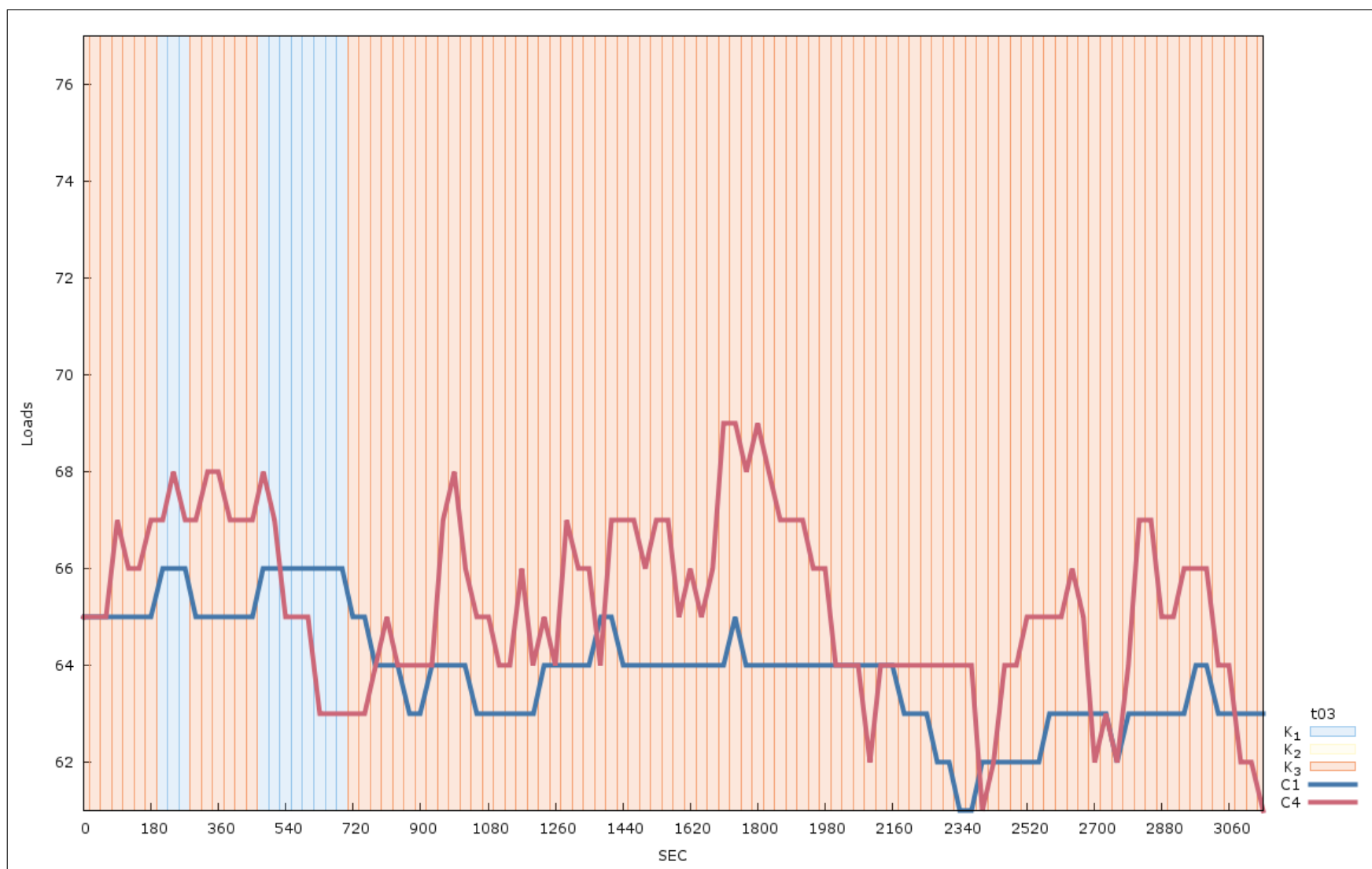


Figure F.6: Trial 3—High-Density Workload—Chiller Clustering on Loads

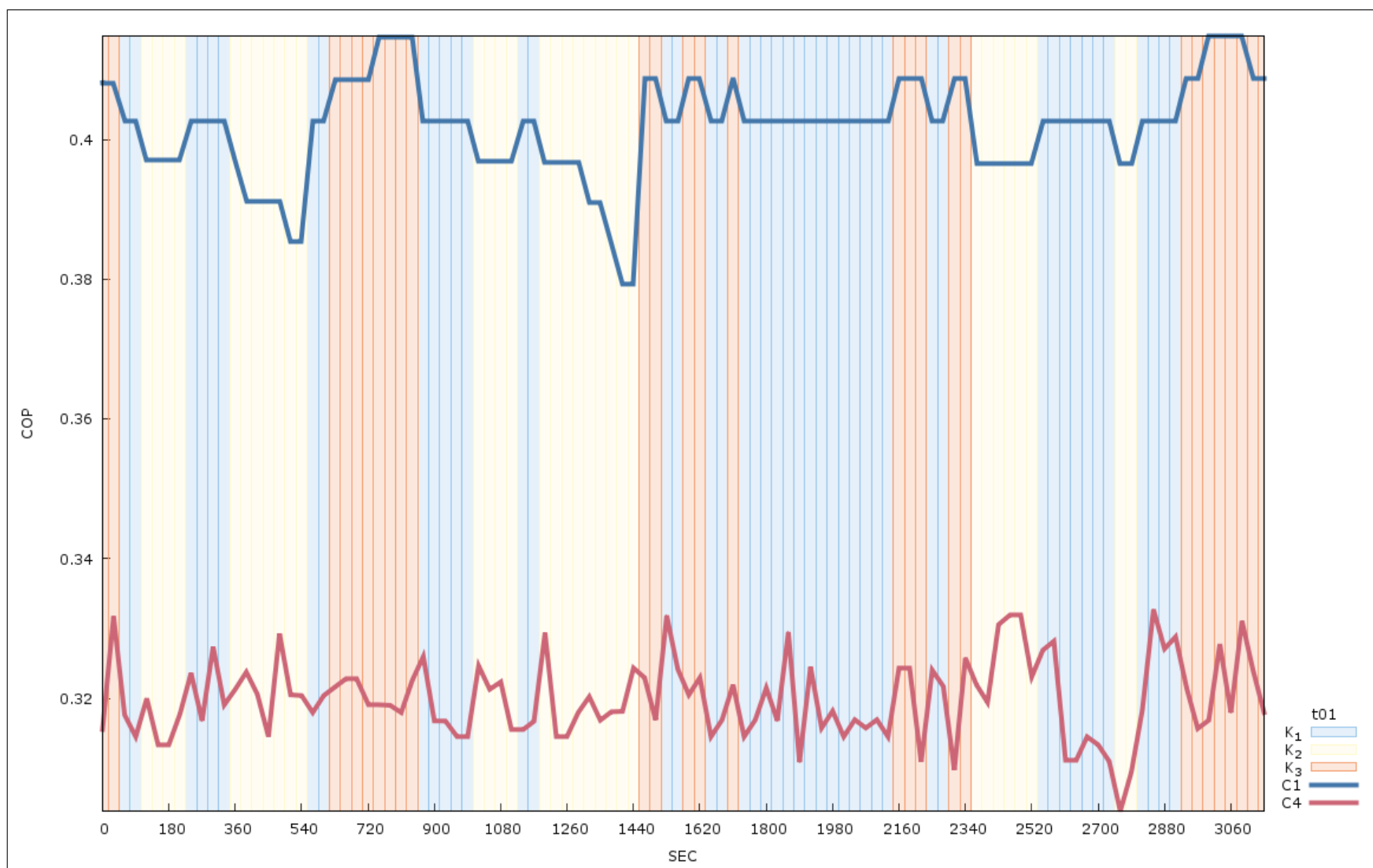


Figure F.7: Trial 1—High-Density Workload—Chiller Clustering on COP

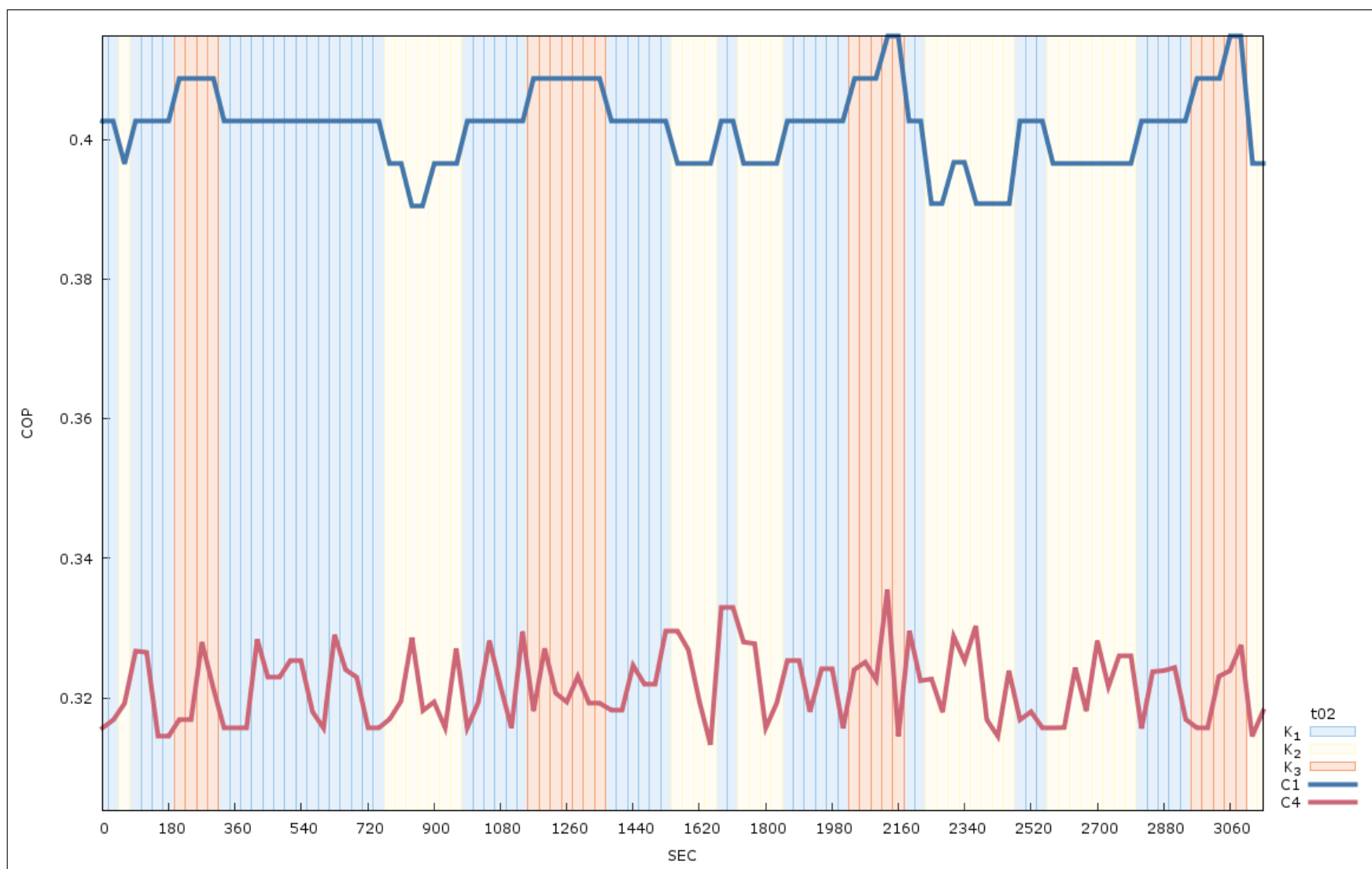


Figure F.8: Trial 2—High-Density Workload—Chiller Clustering on COP

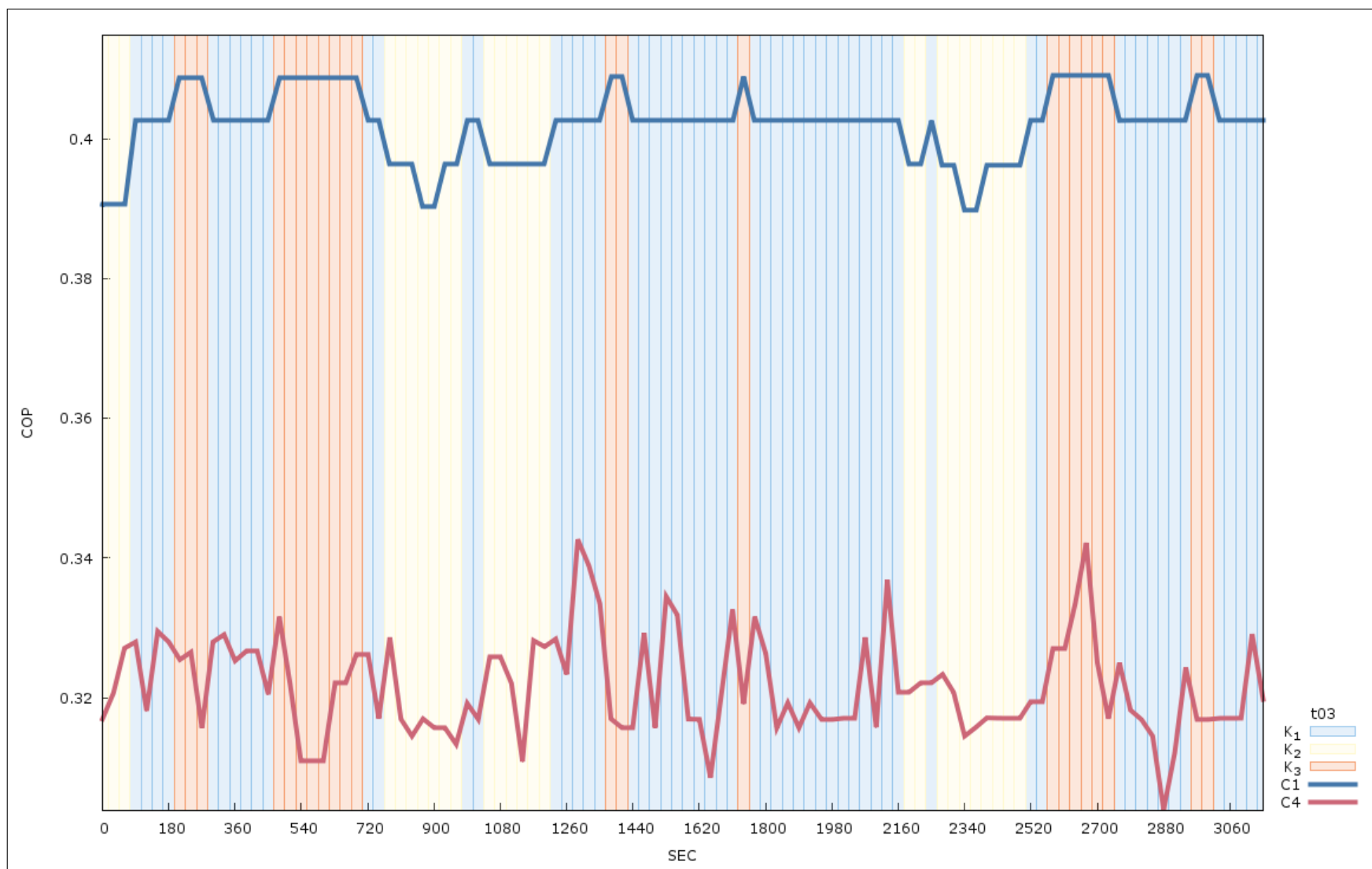


Figure F.9: Trial 3—High-Density Workload—Chiller Clustering on COP

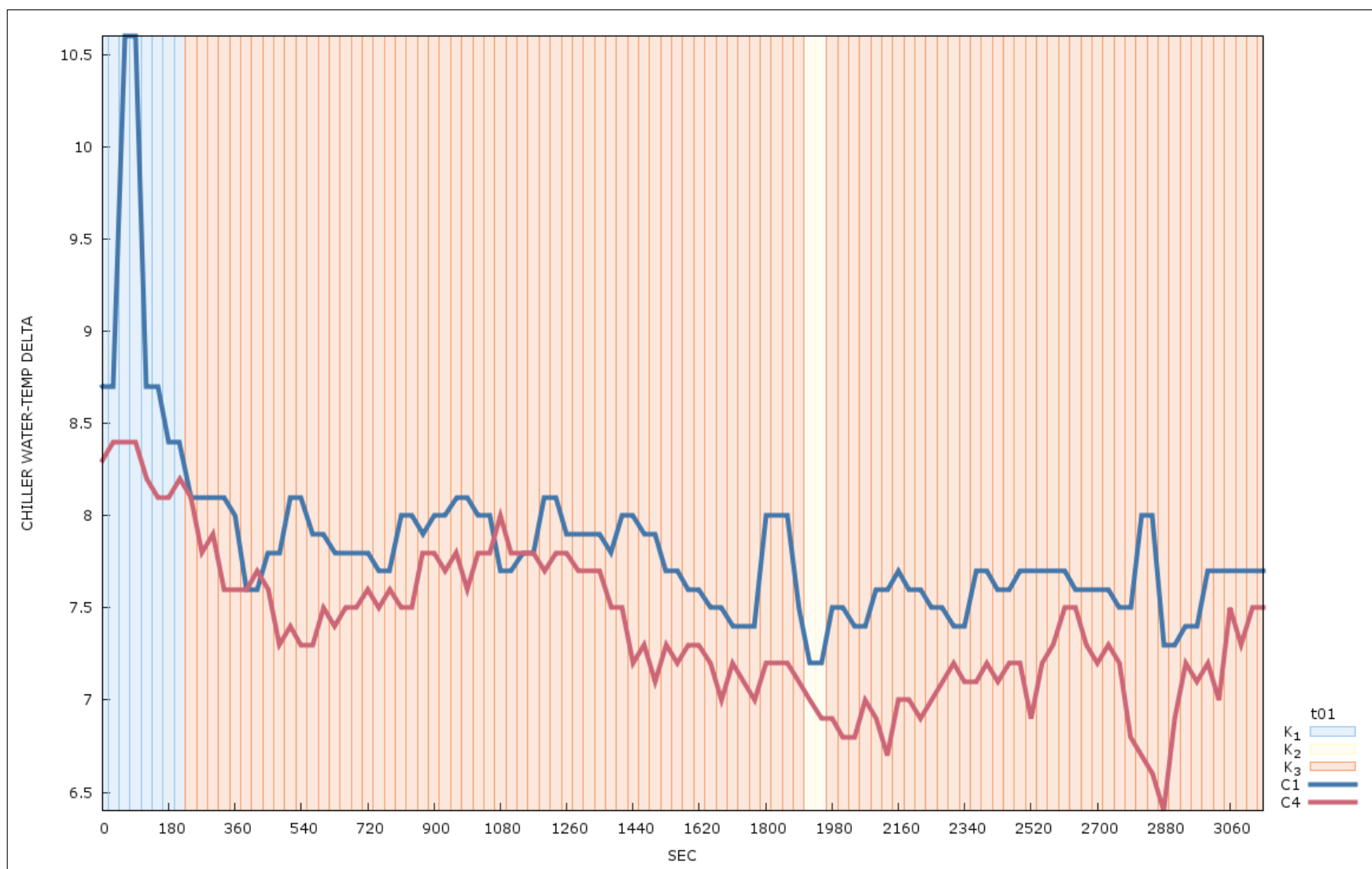


Figure F.10: Trial 1—High-Density Workload—Clustering on Chilled Water Temperature Delta

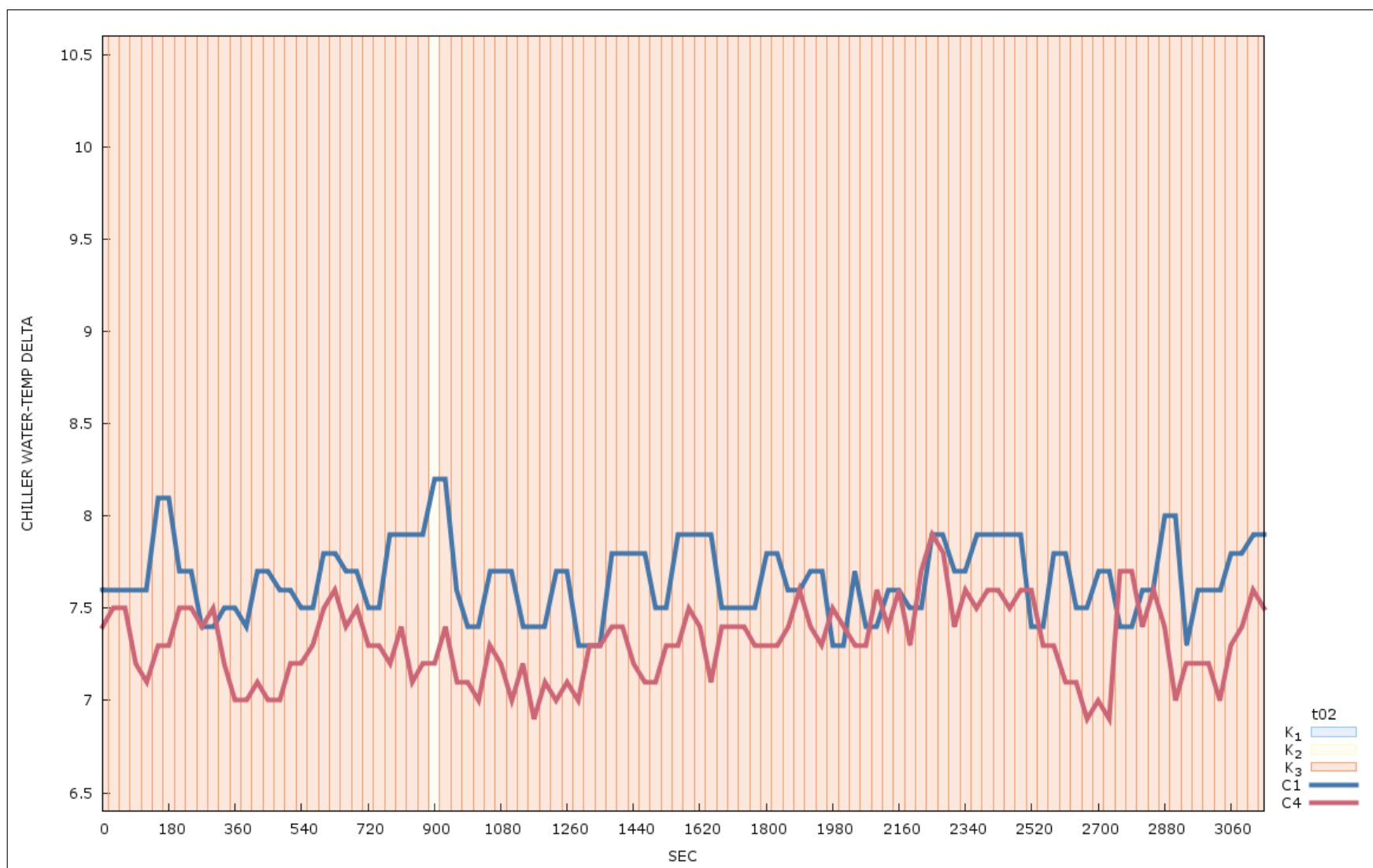


Figure F.11: Trial 2—High-Density Workload—Clustering on Chilled Water Temperature Delta

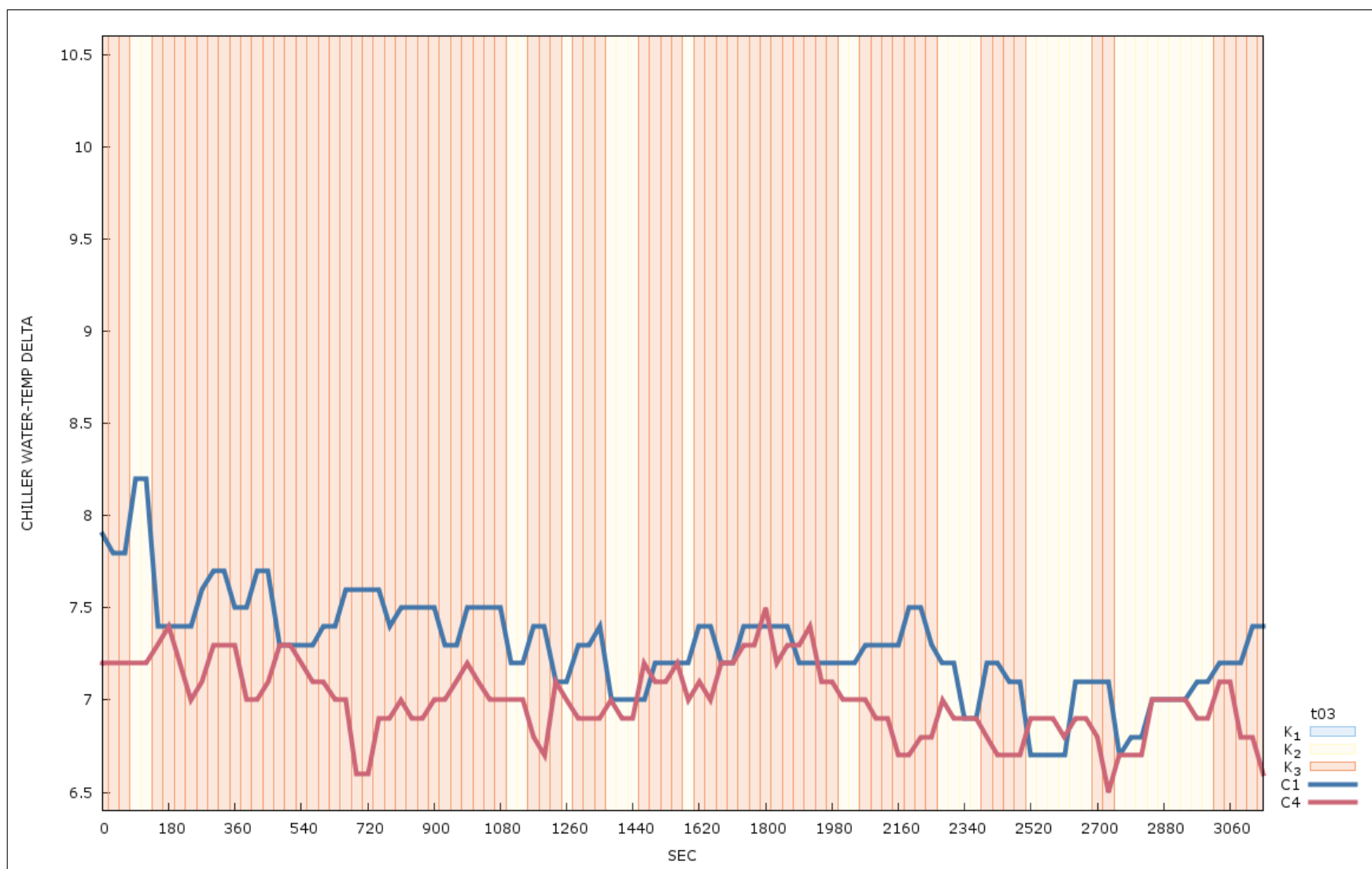


Figure F.12: Trial 3—High-Density Workload—Clustering on Chilled Water Temperature Delta

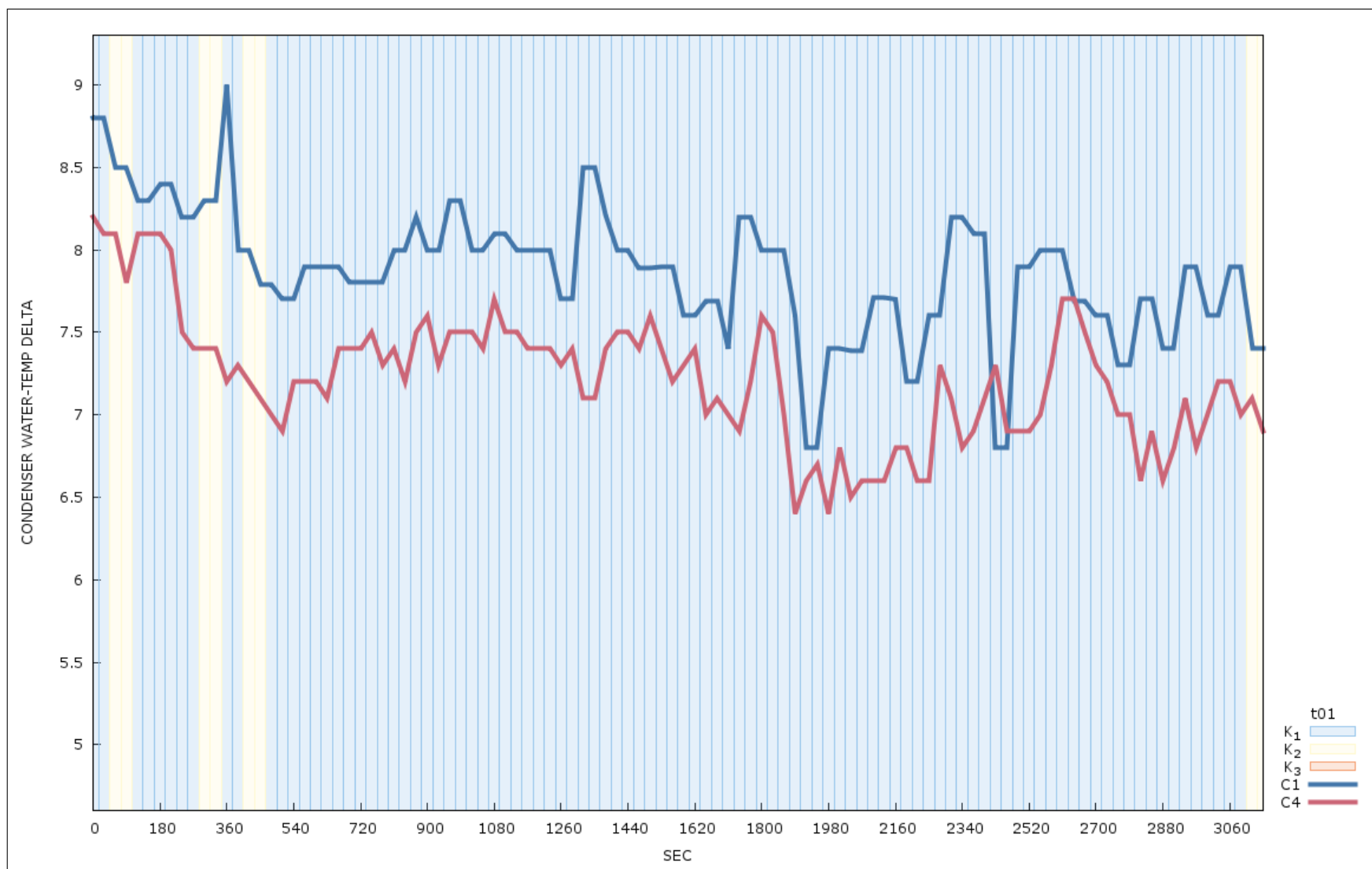


Figure F.13: Trial 1—High-Density Workload—Clustering on Condenser Water Temperature Delta

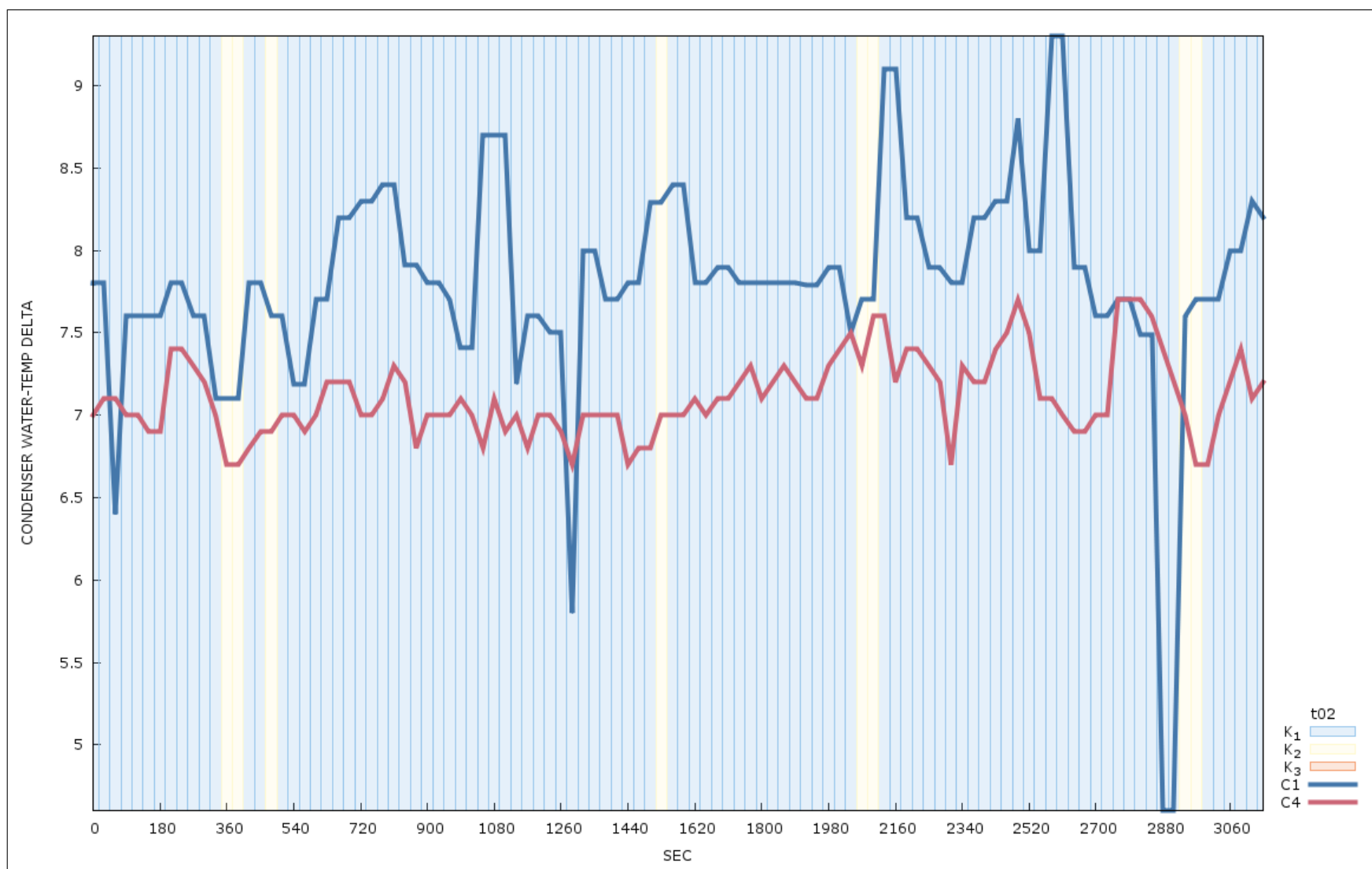


Figure F.14: Trial 2—High-Density Workload—Clustering on Condenser Water Temperature Delta

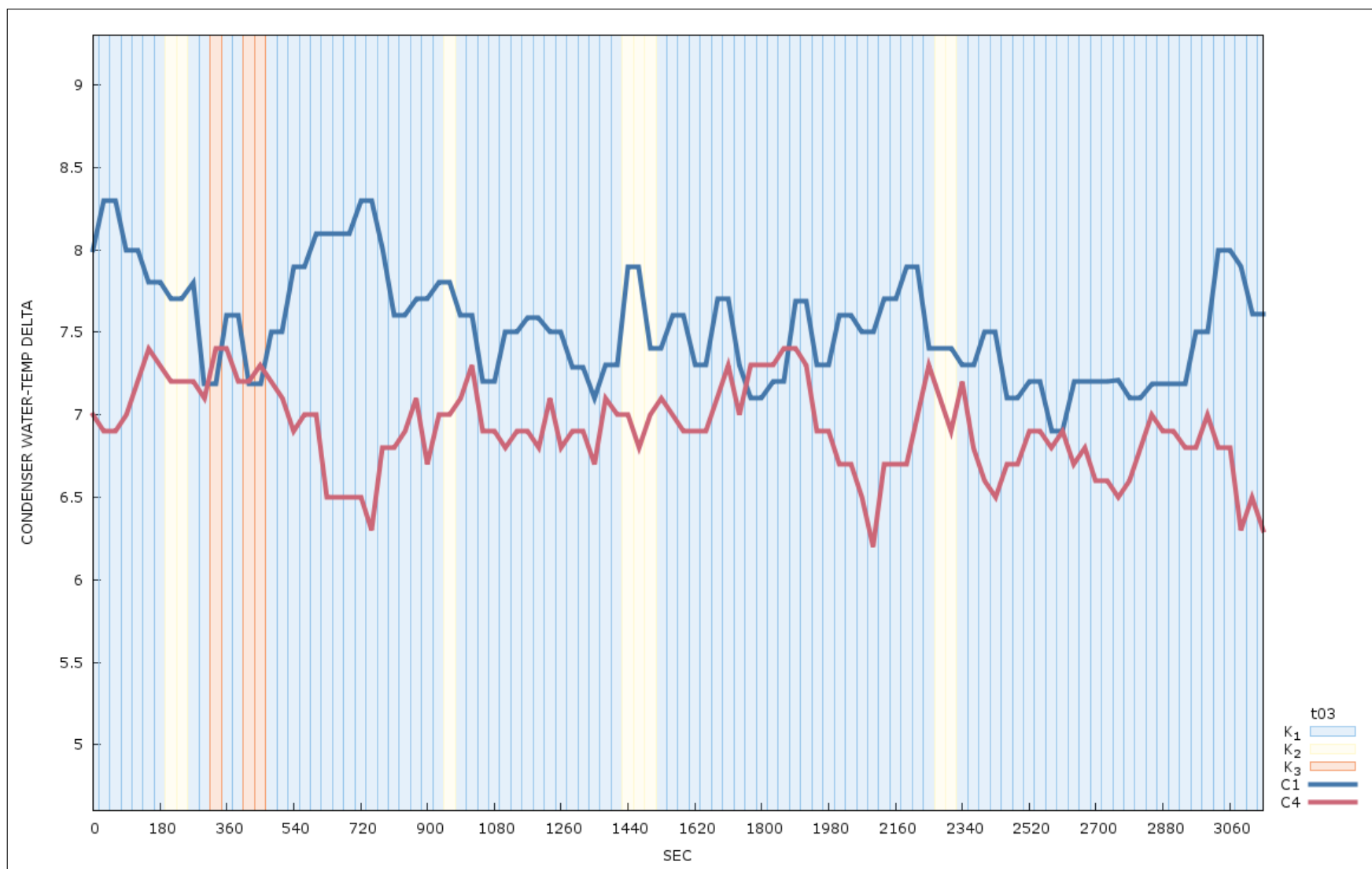


Figure F.15: Trial 3—High-Density Workload—Clustering on Condenser Water Temperature Delta

Bibliography

- [1] Elke Achtert, Ahmed Hettab, Hans-Peter Kriegel, Erich Schubert, and Arthur Zimek. Spatial outlier detection: data, algorithms, visualizations. In *Proceedings of the 12th international conference on Advances in spatial and temporal databases*, SSTD'11, pages 512–516, Berlin, Heidelberg, 2011. Springer-Verlag.
- [2] Rashawn L. Knapp, Karen L. Karavanic, Sriram Krishnamoorthy, and Andres Marquez. Power- and cooling- aware parallel performance diagnosis. In *Parallel and Distributed Computing and Systems (PDCS 2011)*, Dallas, USA, December 2011.
- [3] Debprakash Patnaik, Manish Marwah, Ratnesh Sharma, and Naren Ramakrishnan. Sustainable operation and management of data center chillers using temporal data mining. In *Proceedings of the 15th ACM SIGKDD international conference on Knowledge discovery and data mining*, KDD '09, pages 1305–1314, New York, NY, USA, 2009. ACM.
- [4] Debprakash Patnaik, Manish Marwah, Ratnesh K. Sharma, and Naren Ramakrishnan. Temporal data mining approaches for sustainable chiller management in data centers. *ACM Trans. Intell. Syst. Technol.*, 2(4):34:1–34:29, July 2011.